European Journal of Medicinal Chemistry 174 (2019) 116–129

Contents lists available at ScienceDirect

European Journal of Medicinal Chemistry

journal homepage: http://www.elsevier.com/locate/ejmech

Research paper

Benzoic acid-derived nitrones: A new class of potential acetylcholinesterase inhibitors and neuroprotective agents

Catarina Oliveira [a, 1], Donatella Bagetta [b, c, 1], Fernando Cagide [a], José Teixeira [a, d], Ricardo Amorim [a, d], Tiago Silva [a, d], Jorge Garrido [a, e], Fernando Remião [f], Eugenio Uriarte [g, h], Paulo J. Oliveira [d], Stefano Alcaro [b, c], Francesco Ortuso [b, c, **], Fernanda Borges [a, *]

[a] CIQUP/Department of Chemistry and Biochemistry, Faculty of Sciences, University of Porto, Rua do Campo Alegre s/n, 4169-007, Porto, Portugal
[b] Department of "Scienze della Salute", University "Magna Græcia" of Catanzaro, Campus Universitario "S.Venuta", Catanzaro, Italy
[c] Net4Science Academic Spin-Off, University "Magna Græcia" of Catanzaro, Campus Universitario "S.Venuta", Catanzaro, Italy
[d] CNC—Center for Neuroscience and Cell Biology, University of Coimbra, UC-Biotech, Biocant Park, Cantanhede, 3060-197, Portugal
[e] Department of Chemical Engineering, Superior Institute of Engineering of Porto (ISEP), IPP, Rua Dr. António Bernardino de Almeida, 431, Porto, 4200-072, Portugal
[f] UCIBIO-REQUIMTE, Laboratory of Toxicology, Department of Biological Sciences, Faculty of Pharmacy, University of Porto, Porto, Portugal
[g] Department of Organic Chemistry, Faculty of Pharmacy, University of Santiago Compostela, Santiago de Compostela, Spain
[h] Instituto de Ciencias Químicas Aplicadas, Universidadd Autónoma de Chile, Santiago, Chile

ARTICLE INFO

Article history:
Received 9 March 2019
Received in revised form
10 April 2019
Accepted 10 April 2019
Available online 17 April 2019

Keywords:
Benzoic acid
Nitrones
Spin traps
Alzheimer's disease
Cholinesterase inhibitors
Acetylcholinesterase
Oxidative stress

ABSTRACT

The discovery of new chemical entities endowed with potent and selective acetylcholinesterase (AChE) and/or butyrylcholinesterase (BChE) inhibitory activity is still a relevant subject for Alzheimer's disease therapy. Therefore, a small library of benzoic based amide nitrones (compounds **24** to **42**) was synthesized and screened toward cholinesterase enzymes. SAR studies showed that the *tert*-butyl moiety is the most favourable nitrone pattern. In general, *tert*-butyl derivatives effectively inhibited AChE, being compound **33** the most potent ($IC_{50} = 8.3 \pm 0.3$ μM; *Ki* 5.2 μM). The data pointed to a non-competitive inhibition mechanism of action, which was also observed for the standard donepezil. None of compounds showed BChE inhibitory activity. Molecular modelling studies provided insights into the enzyme-inhibitor interactions and rationalised the experimental data, confirming that the binding mode of nitrones **33** and **38** towards AChE has the most favourable binding free energy.

The *tert*-butylnitrones **33** and **38** were not cytotoxic on different cell lines (SH-SY5Y and HepG2). Moreover, compound **33** was able to prevent *t*-BHP-induced oxidative stress in SH-SY5Y differentiated cells.

Due to its AChE selectivity and promising cytoprotective properties, as well as its appropriate drug-like profile pointing toward blood-brain barrier permeability, compound **33** is proposed as a valid lead for a further optimization step.

© 2019 The Authors. Published by Elsevier Masson SAS. This is an open access article under the CC BY-NC-ND license (http://creativecommons.org/licenses/by-nc-nd/4.0/).

Abbreviations: ACh, Acetylcholine; AChE, acetylcholinesterase; AD, Alzheimer's disease; ATCI, Acetylthiocholine iodide; ATP, adenosine triphosphate; BBB, blood-brain barrier; BCh, butyrylcholine; BChE, butyrylcholinesterase; BTCI, butyrylthiocholine iodide; Ch, choline; ChEIs, cholinesterase inhibitors; ChEs, cholinesterases; clogP, logarithm of the octanol-water partition coefficient; CNS, central nervous system; DIPEA, *N*,*N*-Diisopropylethylamine; DTNB, 5,5′-dithiobis-(2-nitrobenzoate); EDTA, Ethylenediaminetetraacetic acid; FDA, Food and Drug Administration; HBA, number of hydrogen acceptors; HBD, number of hydrogen donors; HBSS, Hank's balanced salt solution; *Ki*, inhibition constant; K_m, Michaelis constant; log BB, blood (plasma)-brain partitioning; NEAA, nonessential amino acids; *n*rotb, number of rotatable bonds; OS, oxidative stress; PCC, pyridinium chlorochromate; ROS, reactive oxygen species; SAR, Structure-Activity Relationship; *t*-BHP, *tert*-butyl hydroperoxide; TNB^{2-}, 5-thio-2-nitrobenzoate anion; TPA, 12-*O*-tetradecanoylphorbol-13-acetate; tPSA, topological polar surface area; V_{max}, maximum velocity.

* Corresponding author. CIQUP/Department of Chemistry and Biochemistry, Faculty of Sciences, University of Porto, Rua do Campo Alegre s/n, 4169-007, Porto, Portugal.
** Corresponding author. Department of "Scienze della Salute", University "Magna Græcia" of Catanzaro, Campus Universitario "S.Venuta", Catanzaro, Italy.
E-mail addresses: ortuso@unicz.it (F. Ortuso), fborges@fc.up.pt (F. Borges).
[1] These authors contributed equally to the work.

https://doi.org/10.1016/j.ejmech.2019.04.026
0223-5234/© 2019 The Authors. Published by Elsevier Masson SAS. This is an open access article under the CC BY-NC-ND license (http://creativecommons.org/licenses/by-nc-nd/4.0/).

1. Introduction

Alzheimer's disease (AD) is the most common type of dementia [1], accounting for up to 70% of cases worldwide [2,3], and being characterized as a multifactorial disease [4–7]. AD is associated with a decrease of cholinergic activity and is also related with increased oxidative stress (OS) [8,9]. Cholinesterases (ChE), a family of enzymes that mainly catalyse the hydrolysis of the neurotransmitter acetylcholine (ACh), are involved in the restoration of the cholinergic pathway at the end of the nerve transmission [9,10]. There are two main types of ChEs identified so far, namely acetylcholinesterase (AChE) and butyrylcholinesterase (BChE): AChE hydrolyses ACh and BChE hydrolyses butyrylcholine (BCh) [10,11]. While AChE prevails in the healthy brain, BChE has a negligible starring role in the regulation of synaptic ACh levels [9,12]. Accordingly, the use of selective AChE inhibitors (AChEI) is an important therapeutic approach for AD. Cholinesterase inhibitors (ChEIs) have shown several benefits including reduced degradation of synaptic ACh, improvement of brain ACh levels in a dose-dependent manner resulting in an enhanced cholinergic transmission in patients with AD and other dementias. However, the drugs currently approved by Food and Drug Administration (FDA) [8,13,14], namely donepezil and galantamine (selective and reversible AChEIs) and rivastigmine (a dual cholinesterase inhibitor, which can inhibit both AChE and BChE) are unable to modify disease progression.

Oxidative stress-related events are also relevant for AD progression. For instance, OS and mitochondrial damage have been associated with AD associated events [4], as the OS redox changes in specific cellular components cause a more oxidized state, bringing about to an augmented production of reactive oxygen species (ROS) and/or less effective intrinsic antioxidant activity [15].

Over the past decade, there have been substantial efforts to design multi-target drugs (MTDs) as a therapeutic solution for AD, an approach that is moved by the increase knowledge that AD is a complex and multifactorial disease affecting many interlinked pathological pathways. In this context, the development of new chemical entities able to prevent and/or minimize OS-related events with remarkable capacities to inhibit ChE activity is still a relevant issue.

Nitrones, a class of compounds known as spin traps, were described as having the ability to stabilize or trap free radicals and reduce the damage associated with unbalanced production of radical reactive species [16,17]. These compounds comprise the general structure R_1-CH=NO-R_2 (Fig. 1a) and the underlying mechanism behind their free radical trapping action is related to their ability to interact with highly reactive oxygen- and carbon-centred radicals ($X^{\bullet}$) yielding nitroxide products (Fig. 1b), which are then stabilized by resonance [18,19].

Following a MTD strategy in the present work we report the design and synthesis of new hybrid nitrones (benzoic based amide nitrones) as potential ChEIs endowed with neuroprotective properties. Structural modifications were performed on the aromatic pattern, spacer length and type of nitrone covalently bound to the carbon flexible aliphatic chain (Fig. 2). All derivatives were

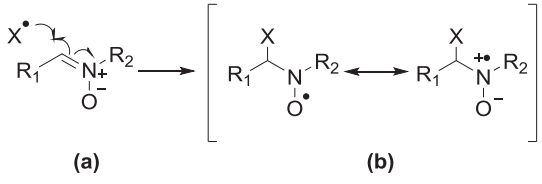

Fig. 1. Free radical trapping mechanism of nitrones.

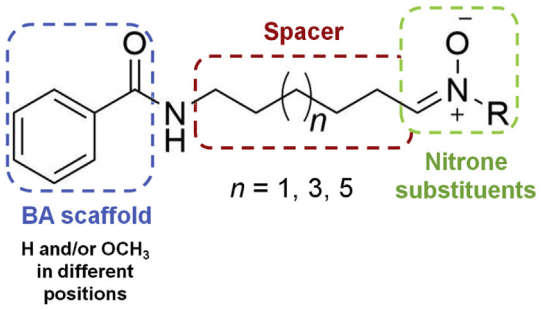

Fig. 2. General structure of novel ChEIs amide nitrones based on benzoic acid (BA).

evaluated for ChEs inhibition, kinetics and mechanism of enzymatic inhibition, cytotoxicity, antioxidant profile in cell-based systems and drug-like properties. In addition, in order to rationalize our results, docking experiments were performed using models built based on the crystal structures of human AChE and BChE.

2. Results and discussion

2.1. Chemistry

The synthesis of novel hybrid nitrones structurally based on benzoic acid was performed following the synthetic strategy depicted in Scheme 1. The compounds were obtained in three synthetic steps using benzoic acid (**1**), 3-methoxybenzoic acid (**2**), 4-methoxybenzoic acid (**3**), 3,4-dimethoxybenzoic acid (**4**) and 3,4,5-trimethoxybenzoic acid (**5**) as starting materials. The first synthetic step consisted of an amidation reaction of benzoic acids **1**–**5** using dissimilar coupling agents, and different length of the linker spacers. Therefore, ethyl chloroformate (step a) was used for the introduction of the 6-aminohexan-1-ol spacer, yielding compounds **6**–**9** and **12**. Alternatively, phosphorus oxychloride (step b) was used with the 8-aminooctan-1-ol and 10-aminodecan-1-ol spacers, yielding derivatives **10**–**11** and **13**–**14**. The following reaction (step c) was the oxidation of the alcohol group of compounds **6**–**14** to the corresponding aldehydes **15**–**23** with pyridinium chlorochromate. Nitrones **24**–**42** were then obtained via a microwave-assisted reaction (step d) using three different hydroxylamines (*N*-*tert*-butylhydroxylamine hydrochloride, *N*-benzylhydroxylamine hydrochloride and *N*-cyclohexylhydroxylamine hydrochloride). Following this strategy, we successfully synthesized a series of derivatives with different aromatic substitution patterns, aliphatic chain length spacers and nitrone moieties.

2.2. Assessment of acetyl and butyrylcholinesterase inhibition

AChE and BChE inhibitory activity of nitrones **24**–**42** was evaluated following the Ellman's method [20,21], with AChE from *Electrophorus electricus* (electric eel, *eel*AChE) and BChE from equine serum (*eq*BChE). Acetylthiocholine iodide (ATCI) or butyrylthiocholine iodide (BTCI) were used as substrates for AChE or BChE, respectively, releasing thiocholine and acetate or butyrate. Then, thiocholine reacts with 5,5′-dithiobis-(2-nitrobenzoate) (DTNB) ion to produce 5-thio-2-nitrobenzoate (TNB^{2-}) anion, which was determined by UV/Vis spectroscopy [20,21], enabling the screening for ChE inhibition after incubation with the test compounds. Donepezil used as standard ChE inhibitor [10] showed a higher potency for AChE than BChE ($IC_{50} = 25 \pm 1$ nM and 2.2 ± 0.2 μM, respectively). The results of the inhibitory potency (IC_{50} values) of compounds under study and standard inhibitor (donepezil) are shown in Table 1.

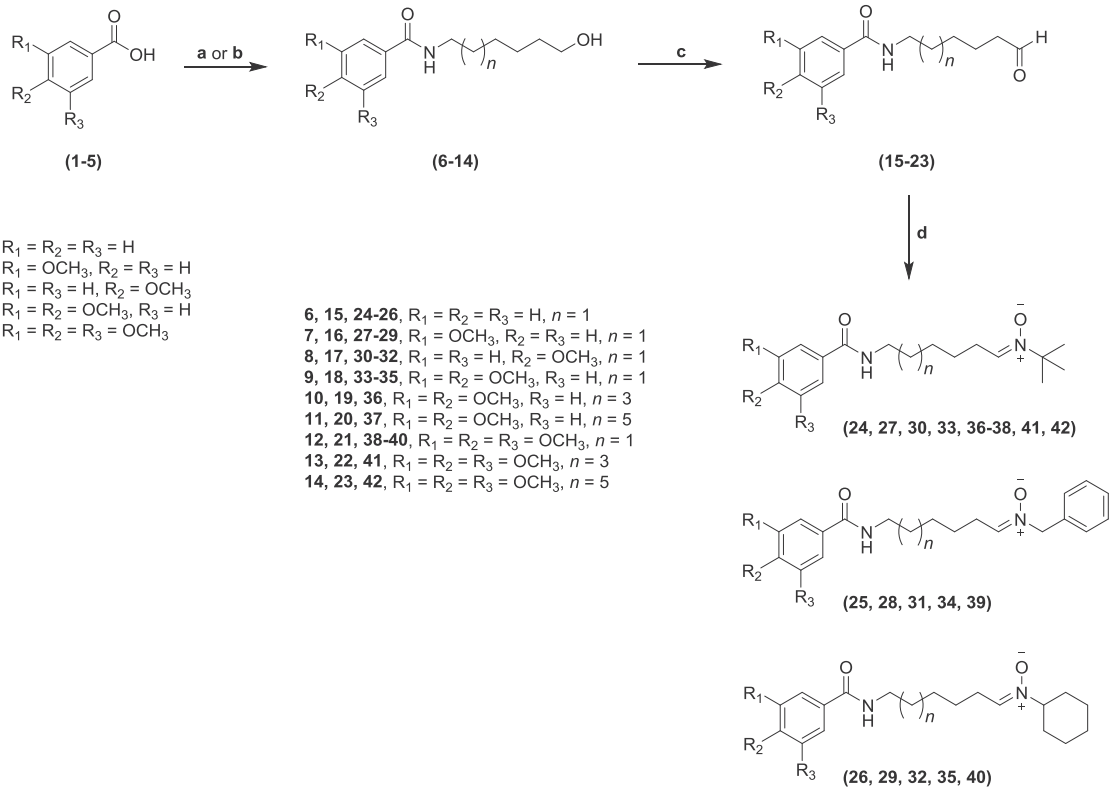

Scheme 1. Synthetic strategy followed to obtain nitrone derivatives **24**–**42** from benzoic acids **1**–**5**. Reagents and conditions: **a.** Et_3N, $ClCOOC_2H_5$, $NH_2(CH_2)_5CH_2OH$, r.t., 10 h; **b.** $POCl_3$, $NH_2(CH_2)_7CH_2OH$ or $NH_2(CH_2)_9CH_2OH$, DIPEA, 1–2 h; **c.** PCC, CH_2Cl_2, 2 h; **d.** $(CH_3)_3CNHOH \cdot HCl$, $C_6H_5CH_2NHOH \cdot HCl$ or $C_6H_{11}NHOH \cdot HCl$, $NaHCO_3$, MW, 90 °C, 10–15 min.

Compounds **27**, **30**, **33**, **36**–**38**, **41** and **42** operated as effective and selective AChEIs. The aromatic ring substituents as well as the spacer length and the nitrone moiety had a significant influence on AChE inhibitory activity. Firstly, the type of substituent of the nitrone group (**24**–**42**) markedly influenced the activity, as only the derivatives bearing a *tert*-butyl group (**27**, **30**, **33**, **36**–**38**, **41** and **42**) were active toward AChE ($IC_{50} = 8.3–27.2\ \mu M$). Curiously, the introduction of benzyl and cyclohexyl nitrone moieties did not lead to the same outcome.

The aromatic ring substituents also had a significant effect on AChE inhibition. Indeed, while benzoic acid derivatives (**24**–**26**) lacked inhibitory activity toward AChE, the introduction of methoxy groups led to an enhancement of the inhibitory effect. Although the introduction of *m*- or *p*-OCH_3 substituents (compounds **27** and **30**) led to similar inhibitory potencies ($IC_{50} = 27.2 \pm 2.9$ and $26.1 \pm 2.7\ \mu M$, respectively), a significant improvement was observed for the 3,4,5-trissubstituted derivative **38** ($IC_{50} = 17.2 \pm 1.3\ \mu M$) and, in particular, for the 3,4-dimethoxy derivative **33** ($IC_{50} = 8.3 \pm 0.3\ \mu M$).

Then, we studied the effect of the length of the alkyl linker for the derivatives with optimal aromatic patterns (3,4-dimethoxy and 3,4,5-trimethoxy) and nitrone moiety (*tert*-butylnitrone). Accordingly, the spacer was replaced by an eight- and ten-carbon chain. It was observed that the increase of the spacer for the 3,4-OCH_3 derivatives (compounds **36** and **37**) did not progress the inhibitory potency but for 3,4,5-OCH_3 derivatives (compounds **41** and **42**) although a slight improvement of inhibitory activity was noticed, reaching a mild 1.5-fold increase for nitrone **42** ($IC_{50} = 11.8 \pm 0.8\ \mu M$), which had a ten-carbon spacer.

As none of the precursors (**1**–**5**) were active against AChE at the highest concentration tested (50 μM) it can be concluded that the presence of a positively charged terminal nitrogen (*tert*-butylnitrone) and an alkyl spacer is required for activity. Moreover, nitrones are selective for AChE as none of the compounds (nitrones and precursors) showed inhibitory activity for BChE at the highest concentration tested (50 μM).

2.3. Assessment of drug-like properties

The drug-like properties were determined for all the nitrone derivatives (**24**–**42**), donepezil and precursors **1**–**5** (see SI). The calculated parameters encompassed: molecular weight (MW), partition coefficient (clog P), topological polar surface area (tPSA in $Å^2$), number of hydrogen acceptors (HBA), number of hydrogen donors (HBD), number of rotatable bonds (*n*rotb) and blood (plasma)-brain partitioning (logBB) (Table 2).

For nitrones with *tert*-butyl moiety (**27**, **30**, **33**, **36**–**38**, **41** and **42**, Table 2), we observed that the values of HBA and HBD were in agreement with the drug-likeness requirements of the Linpinski's "Rule of 5" (with HBA < 10 and HBD < 5) [22]. In general, all compounds exhibited a clogP value lower than 5, with the clogP values ranging from 2.59 to 5.05, which is within the optimal range for orally administered and central nervous system (CNS) drugs [22,23]. However, comparing with CNS^+ drug parameters, compounds **38**, **41** and **42** displayed a value of HBA = 7, which is out of the proposed range.

The prediction of blood-brain barrier (BBB) permeability, determined by the logBB (the ratio of the steady-state concentrations of the drug in the brain and in the blood) was also assessed. Compounds with logBB below −1 are poorly distributed to the brain and are improbable to operate as effective CNS drugs [24]. All nitrones depicted on Table 2 displayed logBB > −1, pointing towards potential BBB permeability.

Table 1
AChE and BChE inhibitory activity (IC_{50}) of nitrone derivatives **24**–**42** and donepezil.

Compound	Structure	IC_{50} (μM ± SD)	
		*eel*AChE	*eq*BChE
24	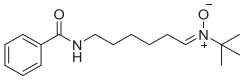	a	a
25	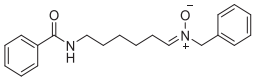	a	a
26	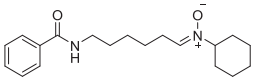	27.2 ± 2.9	a
27	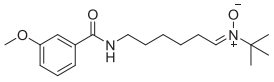	a	a
28	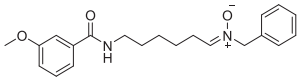	a	a
29	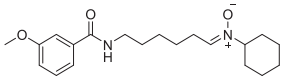	26.1 ± 2.7	a
30	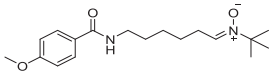	a	a
31	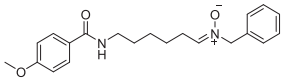	a	a
32	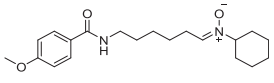	8.3 ± 0.3	a
33	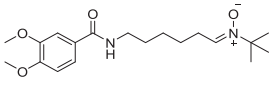	a	a
34	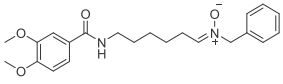	a	a
35	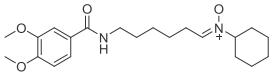	12.2 ± 0.4	a
36	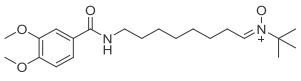	12.6 ± 0.6	a
37	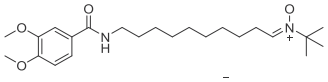	17.2 ± 1.3	a
38	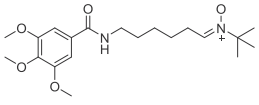	a	a
39	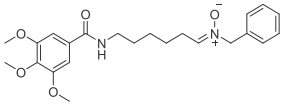	a	a
40	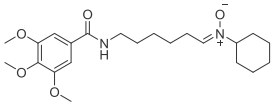	16.9 ± 1.3	a

(*continued on next page*)

Table 1 (*continued*)

Compound	Structure	IC_{50} (μM ± SD)	
		*eel*AChE	*eq*BChE
41	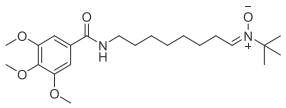	11.8 ± 0.8	[a]
42	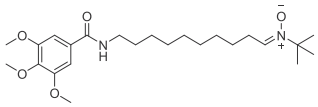	0.025 ± 0.001	2.2 ± 0.2
Donepezil	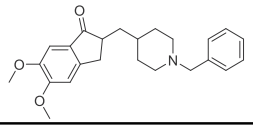		

[a] Inactive at 50 μM (highest concentration tested).

Table 2
Drug-like properties of nitrones derivatives with *tert*-butyl moiety (**27**, **30**, **33**, **36**–**38**, **41** and **42**).

Compound	MW[a]	clog P[a]	tPSA (Å^2)[a]	HBA[a]	HBD[a]	*n*rotb[a]	log BB[a]
27	320.4	2.99	67.08	5	1	10	0.232
30	320.4	2.99	67.08	5	1	10	0.232
33	350.5	2.80	76.31	6	1	11	0.086
36	378.5	4.15	76.31	6	1	13	0.109
37	406.6	5.05	76.31	6	1	15	0.115
38	380.5	2.59	85.54	7	1	12	0.004
41	408.5	3.94	85.54	7	1	14	0.028
42	436.6	4.85	85.54	7	1	16	0.035
CNS$^+$ drugs [7,25-28]	< 450	< 5	< 60-70	< 7	< 3	< 8	≥ −1

MW: molecular weight; clog P: logarithm of the octanol-water partition coefficient; tPSA: topological polar surface area; HBA: number of hydrogen acceptors; HBD: number of hydrogen donors; *n*rotb: number of rotatable bonds; log BB: logarithm of the ratio of the concentration of a drug in the brain and in the blood.
[a] Properties calculated using StarDrop software.

2.4. Modelling studies

To study the influence of the nitrone substituents on *h*ChEs molecular recognition, compounds **27**–**35** and **38**–**40** were submitted to molecular docking simulations and the resulting theoretical complexes were scored using the Molecular Mechanics/Generalized Born Surface Area (MM-GBSA) binding free energy estimation [29]. Differently from which was observed for *h*BChE, all evaluated compounds in *h*AChE assumed an extended conformation. The reason of this different behaviour could be related to the known structural differences between the two isoenzymes active sites [30,31] (Fig. S1). Indeed, overlapping *h*BChE poses into the *h*AChE pocket, it was observed that the aromatic residues Phe295, Phe297 and Tyr337 prevented the ligand folded conformation. In fact, these amino acids, in *h*BChE, are replaced by Leu286, Val288 and Ala328, respectively, resulting in less steric hindrance. Although the studied compounds were able to bind the active site of both isoforms their binding free energies suggested for the *tert*-butyl derivatives **27**, **30**, **33**, **38** a *h*AChE preference over *h*BChE (Table 3), with nitrones **33** and **38** as the most energetically favourite *h*AChE ligands, which are in a qualitative agreement with the experimental data.

In particular, into the *h*AChE active site compounds **33, 27**, **30**, and **38** (Figs. 3, S2–S4, respectively) shared both the orientation of the *tert*-butyl group towards the inner side of the gorge and established hydrogen bond to Phe295 backbone by means of the amide oxygen. Into the *h*AChE, stacking interactions with the external Trp286 further stabilized **27**, **33** and **38** complexes.

The corresponding benzyl derivatives **28**, **31**, **34** (Figs. S5–S7) equally interacted with Phe295 and Trp286 and maintained the same orientation. On the contrary, 3,4,5-trimethoxy phenyl ring of the derivative **39** was positioned near the internal Trp86. Nevertheless, this compound performed hydrogen bond to Phe295 backbone by the nitrone oxygen, and its benzyl ring was oriented towards the Trp286 (Fig. S8). Thus, both the number and position of the methoxy group(s) at the aromatic ring and the *tert*-butyl/benzyl substituents seemed to have the same influence on the *h*AChE interactions.

Regarding the cyclohexyl ring substituted derivatives **29**, **32**, **35** and **40** (Figs. S9–S12), it was observed that **29** and **35**, conversely to their *tert*-butyl analogues, respectively directed the 3-methoxy and 3,4-dimethoxy phenyl ring towards to the internal Trp86

Table 3
Ligands-target theoretical binding free energy (in kcal/mol).

Compound	*h*AChE	*h*BChE
27	−49.78	−36.43
28	−42.71	−39.04
29	−35.63	−38.07
30	−44.57	−25.81
31	−39.26	−28.15
32	−38.11	−13.07
33	−50.66	−16.72
34	−39.98	−34.92
35	−35.62	−36.00
38	−52.90	−33.84
39	−25.37	−31.06
40	−33.25	−36.91
(*R*)-Donepezil	−69.65	−44.45
(*S*)-Donepezil	−72.81	−39.22

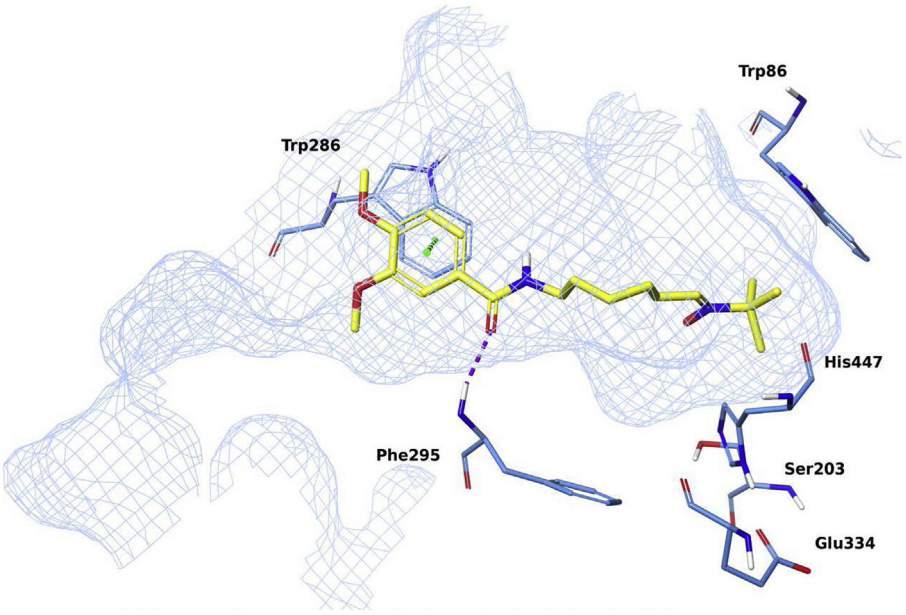

Fig. 3. Best docking pose of compound **33** into *h*AChE active site displayed as light blue mesh. The most relevant interacting residues and the ligand are respectively depicted in light blue and yellow tubes. Stacking interactions and hydrogen bonds are respectively represented in green and purple.

establishing stacking interactions, while the hydrogen bond with Phe295 was established by the nitro group oxygen, similarly to compound **39**. Contrariwise, the binding modes of **32** and **40** were similar with those observed for **30** and **38**.

Therefore, docking findings indicated that all studied compounds were able to bind to *h*AChE active site mainly interacting with Trp286 and Phe295, belonging to the peripheral anion site (PAS) and to the acyl pocket, respectively, which play a key role in ligand binding and specificity [32,33].

However, according to the biological data attained with the nitrone group substituted by benzyl (**28**, **31**, **34**, **39**) and cyclohexyl moieties (**29**, **32**, **35**, **40**) were endowed with a worst *h*AChE binding free energy compared to the corresponding *tert*-butyl analogous. Analysing each MM-GBSA term contributing to the binding free energy definition it was observed that the solvation free energy (Generalized Born electrostatic solvation energy) mostly penalized the benzyl and cyclohexyl derivatives (Table S2).

Focusing on the *h*BChE complexes, as previously reported, these inhibitors showed a folded conformation not dependent from the substituent at the phenyl and nitro moieties. Specifically, the *tert*-butyl derivatives **27**, **30** and **38** (Figs. S13–S15) respectively oriented the 3-methoxy, 4-methoxy and 3,4,5-trimethoxyphenyl ring towards the Phe329 performing stacking contacts, while the 3,4-dimethoxyphenyl ring of **33** interacted to Tyr332 (Fig. S16).

Concerning the benzyl derivatives, the docking poses of **28** (Fig. S17) and **34** (Fig. S18) were quite similar to the **31** (Fig. S19) and **39** (Fig. S20) ones. In particular, **28** and **31** directed the methoxyphenyl ring towards the Tyr332 and the benzyl one towards the Trp231; in the docking geometries of **34** and **39** such moiety was arranged in an opposite manner.

Similar configuration of **34** and **39** was observed for the cyclohexyl derivatives **29**, **35** and **40** (Figs. S21-S23). Instead, regarding **32** both the 4-methoxyphenyl and cyclohexyl ring were located near to Tyr231 and no productive interactions were observed (Fig. S24). Finally, **27**, **30**, **31, 39** and **40** poses highlighted steric hindrance penalties with the residues of the catalytic triad, which could disfavour the *h*BChE recognition. Any issue related with Pan Assay INterference compoundS (PAINS) was found for the compounds under study.

2.5. Assessment of enzyme-inhibition mechanism

To evaluate the inhibition mechanism of the most promising AChEIs (compounds **33** and **38**) kinetic experiments were performed. For this purpose, the enzyme inhibition kinetics was evaluated using different substrate concentrations (ATCI), in absence or presence of compounds **33**, **38** and donepezil at different concentrations. The results are shown in Fig. 4. Graphical analyses of the reciprocal Lineweaver-Burk plots were used to determine Michaelis-Menten reaction kinetic parameters (Michaelis constant, K_m and maximum velocity, V_{max}).

Concerning compound **33**, it was found that the V_{max} decreased while K_m appears to remain unchanged (Fig. 4A), displaying a series of converging lines on the same point of the x-axis (1/[S]). The data pointed to a non-competitive inhibition mechanism of action, which was also observed for the standard donepezil (Fig. 4C), as expected [34,35]. The Lineweaver-Burk plots obtained for compound **38** (Fig. 4B) presented a series of converging lines displaying a behaviour corresponding to a mixed inhibition, which is characterized by the decrease of V_{max} and K_m. Actually, a mixed inhibitor can hinder the binding of substrate and decrease the turnover number of the enzyme [36].

From the Dixon plots, obtained from the replots of the slopes of the Lineweaver-Burk plots *vs.* Inhibitor concentrations (Fig. 4, upper right corners), the AChE inhibition binding affinities, determined as inhibition constants (*Ki*), were calculated. Compounds **33** (Fig. 4A) and **38** (Fig. 4B) displayed *Ki* values of 5.2 and 10.4 μM, respectively. The *Ki* values of compounds **33** ($IC_{50} = 8.3$ μM) and **38** ($IC_{50} = 17.2$ μM) correlated well with their experimental IC_{50}, displaying IC_{50} and *Ki* values slightly equal. Donepezil showed a similar behaviour ($Ki = 16.4$ nM and $IC_{50} = 24.6$ nM, Fig. 4C).

2.6. Assessment of cytotoxicity

The cytotoxic profile of the compounds **24**–**42** (see SI and Fig. 5) was determined by measuring the cellular viability, in human

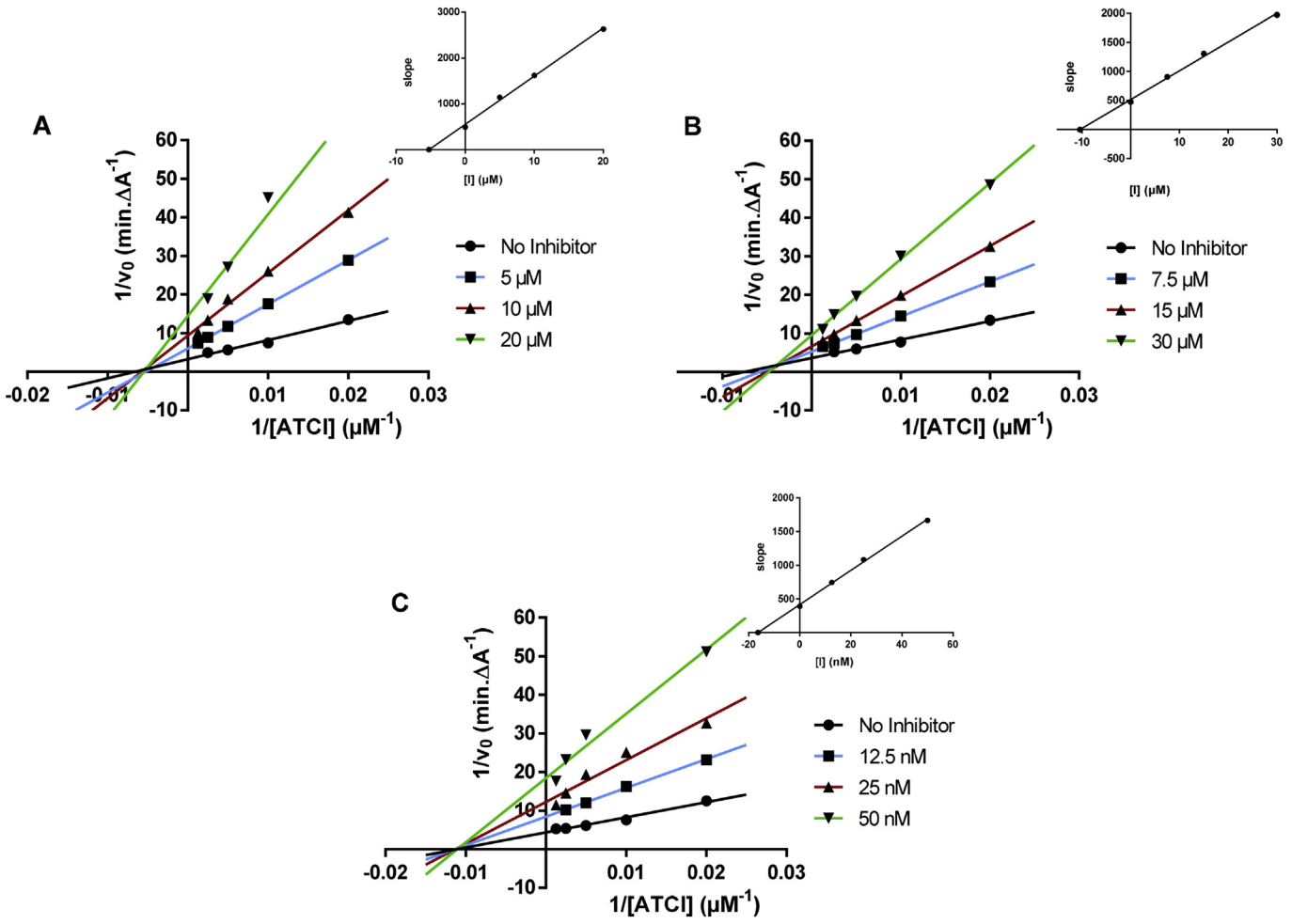

Fig. 4. Kinetic studies on the mechanism of AChE inhibition by **(A)** compounds **33** and **(B) 38**, and **(C)** donepezil. Details in reference [39].

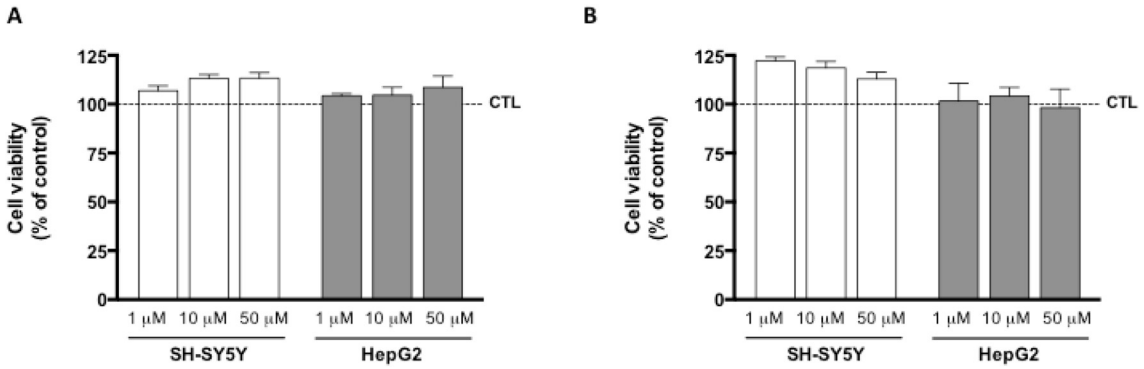

Fig. 5. Cellular viability of human neurablastoma SH-SY5Y and human hepatocarcinoma HepG2 cells after a 24 h treatment with three different concentrations (1, 10 and 50 μM) of nitrone compounds **(A) 33** and **(B) 38**. Cellular viability was evaluated through variations in cell metabolic activity using two methods: MTT and resazurin reduction assays in differentiated SH-SY5Y and HepG2 cells, respectively. Untreated cells were used as control. Results are expressed as mean % of untreated controls ± SEM. (n = 4).

differentiated neuroblastoma (SH-SY5Y cell line) and hepatocarcinoma (HepG2) cells, after a 24 h incubation period at three different concentrations (1, 10 and 50 μM). Both cell lines are often used in the preclinical safety assessment of CNS drug candidates [37]. Cellular viabilities were estimated through the capability of living cells to metabolically reduce MTT and resazurin to formazan and resorufin, respectively, providing an indirect measure of metabolic function [38]. The results obtained are shown in Fig. 5.

In general, the most promising compounds **33** (Fig. 5A) and **38** (Fig. 5B) with *tert*-butyl nitrone moiety did not exhibit a cytotoxicity toward SH-SY5Y and HepG2 cells for all tested concentrations. Interestingly, these compounds slightly increased cell viability (106.8–122.1%) for all tested concentrations in differentiated SH-SY5Y cells, an effect that was not observed in HepG2 cells.

In brief, the data showed that the nitrone derivatives under study did not display significant toxicity effects neither in human SH-SY5Y nor HepG2 cells at concentrations in which they exhibited AChE inhibitory activities, revealing a satisfactory safety window.

2.7. Assessment of OS-induced cell death prevention

The antioxidant properties of the most promising nitrone compounds (**33** and **38**) against OS-induced cell damage were evaluated in SH-SY5Y differentiated cells, at 10, 50, 100 μM. Two different strategies were used: a) the tested compounds were pre-incubated for 24 h at non-cytotoxic concentrations, and then pro-oxidant agents were added to the cell culture; and b) the pro-oxidant agents were first added to the cell culture and then the tested compounds were incubated for 24 h, at non-cytotoxic concentrations (Fig. 6A).

In the present study, classical pro-oxidant agents were used: hydrogen peroxide (H_2O_2), *tert*-butyl hydroperoxide (*t*-BHP), the mitochondrial inhibitors rotenone and antimycin A (ROT/AA), and the anti-cancer agent doxorubicin (DOX). The selected oxidative

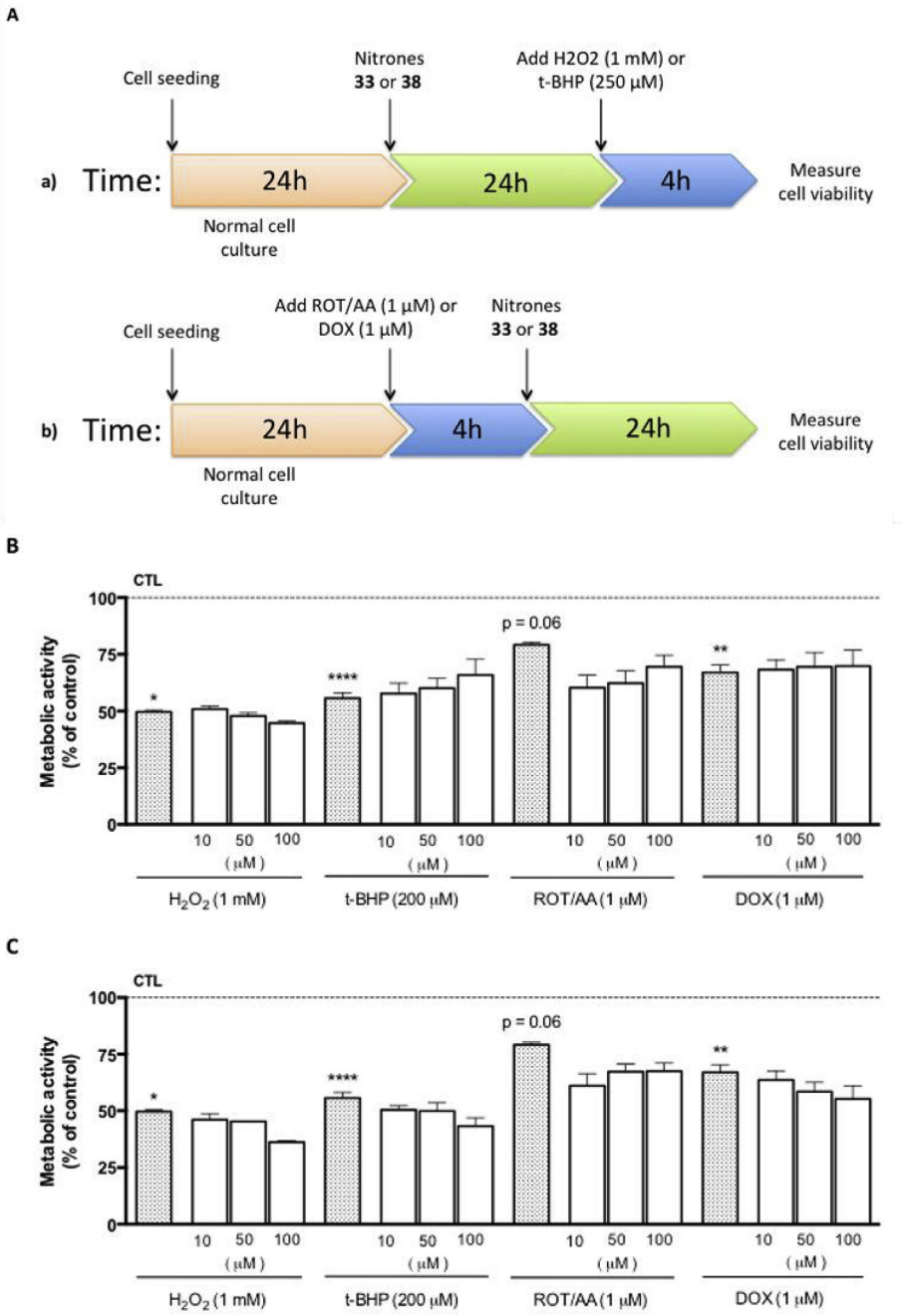

Fig. 6. Antioxidant cytoprotective effects of *tert*-butyl nitrones, **33** and **38**. **(A)** Schematic representation of strategies used to evaluate nitrones' antioxidant properties. Antioxidant activity of compounds **(B) 33** and **(C) 38**, were evaluated in human neuroblastoma SH-SY5Y cells against H_2O_2-, *t*-BHP-, ROT/AA-, and DOX-induced decrease in cell metabolic activity. The comparisons were performed by using one-way ANOVA between the control (oxidative stressors) *vs.* Nitrones under study when were incubated. Data are means ± SEM of four independent experiments and the results are expressed as percentage of control (control = 100%), which represents the cells without any treatment in the respective time point. Significance was accepted with * $P < 0.05$, ** $P < 0.01$, **** $P < 0.0001$.

stressors induced oxidative events by different mechanisms: H_2O_2 is a product of enzymatic activity and dopamine oxidation and can be converted into hydroxyl radicals via Fenton-like reactions [15]; *t*-BHP is an organic peroxide that causes lipid peroxidation, opening of mitochondria nonspecific Ca^{2+}-dependent pore, and cell death [39]; ROT/AA are inhibitors of the mitochondrial electron transport chain, resulting in a burst of superoxide anion production and induction of a ROS-dependent cell damage cascade events; and DOX is a chemotherapeutic drug which generates a redox cycle at different dehydrogenases, including mitochondrial complex I, leading to superoxide anion production, and consequently to mitochondrial dysfunction. Cells treated with H_2O_2 (1 mM, Fig. 6B), *t*-BHP (250 μM, Fig. 6B), ROT/AA (1 μM, Fig. 6B), and DOX (1 μM, Fig. 6B) caused a significant reduction, of about 50.3 ± 1.1%, 44.3 ± 6.4%, 20.7 ± 2.1% and 32.9 ± 6.7%, respectively, in cell metabolic activity when compared with nontreated cells.

In general, none of the promising AChEIs showed remarkable antioxidant effects (Figs. 6B and C). However, compound **33** was able to prevent the *t*-BHP-induced cell damage in a dose-dependent manner (Fig. 6B), a property that can be enhanced after a subsequent optimization step.

3. Conclusions

The development of new benzoic based amide nitrones (compounds **24**–**42**), with different nitrone substituents (*tert*-butyl, benzyl and cyclohexyl), was successfully achieved. The compounds were screened toward cholinesterase enzymes and SAR studies showed that the *tert*-butyl moiety is the most favourable nitrone pattern. Only compounds with the *tert*-butyl moiety (**27**, **30**, **33**, **36**, **38**, **41** and **42**) displayed significant AChE inhibitory activity. Moreover, the presence and number of methoxy substituents, as well as the spacer length, were found to be important contributors for AChEI modulation potency. Compound **33**, with two methoxy functions and a six-carbon aliphatic chain, presented the best inhibitory activity toward AChE (IC_{50} = 8.3 ± 0.3 μM; *Ki* 5.2 μM). The data pointed to a non-competitive inhibition mechanism of action, which was also observed for the standard donepezil. None of compounds showed BChE inhibitory activity.

Molecular modelling studies provided insights into enzyme-inhibitor interactions and a rationale for the selectivity and potency was observed, confirming that nitrones **33** and **38** resulted in the most energetically favourable *h*AChE ligands.

The most promising *tert*-butylnitrones **33** and **38** slightly increased the cell viability (106.8–122.1%) for all tested concentrations in differentiated SH-SY5Y cells and did not have a significant effect on the cellular viability in HepG2 cells. Nitrone derivatives **33** and **38** revealed a satisfactory safety window as they did not display toxic effects in both cell lines. Furthermore, compound **33** was able to prevent the *t*-BHP-induced cell damage in a dose-dependent manner in SH-SY5Y differentiated cells, a property that can be enhanced after a subsequent optimization step.

Due to its AChE selectivity and promising cytoprotection properties, as well as its appropriate drug-like properties, pointing towards BBB permeability compound **33** is proposed as a valid lead for further optimization step.

4. Experimental section

4.1. Chemistry

4.1.1. Synthesis of benzoic acid-derived nitrones

4.1.1.1. General procedures to obtain benzamide derivatives (6–14). ***A1)*** The appropriate benzoic acid (benzoic acid (**1**), 3-methoxybenzoic acid (**2**), 4-methoxybenzoic acid (**3**), 3,4-dimethoxybenzoic acid (**4**) or 3,4,5-trimethoxybenzoic acid (**5**), 1 mmol), was dissolved in dichloromethane (40 mL) and triethylamine (2 mmol) was added. Then, ethyl chloroformate (2 mmol) was added dropwise to the stirred solution kept in an ice bath. After stirring 2 h at room temperature, the mixture was cooled again and the 6-aminohexan-1-ol (2 mmol) was added. The purification conditions are described in literature [15,39].

A2) The appropriate benzoic acid (3,4-dimethoxybenzoic acid (**4**) or 3,4,5-trimethoxybenzoic acid (**5**), 1 mmol) was dissolved in dichloromethane (15 mL) and $POCl_3$ (1 mmol) was added at room temperature. After 30 min, the reactional mixture was cooled (ice bath) and 8-aminooctan-1-ol or 10-aminodecan-1-ol (1.2 mmol) and DIPEA (4 mmol) were added. The reaction was stirred for 1–2 h at room temperature. The purification conditions are described in literature [15].

***N*-(6-Hydroxyhexyl)benzamide (6).** Procedure A1. η = 81%. ^{1}H NMR ($CDCl_3$): δ = 1.40–1.42 (4H, *m*, $N(CH_2)_2(C\underline{H}_2)_2$), 1.54–1.66 (4H, *m*, $NCH_2C\underline{H}_2(CH_2)_2C\underline{H}_2$), 1.77 (1H, *s*, OH), 3.42–3.47 (2H, *m*, NCH_2), 3.63 (2H, *t*, *J* = 6.5 Hz, CH_2O), 6.28 (1H, *s*, NH), 7.39–7.43 (2H, *m*, H(3) and H(5)), 7.46–7.50 (1H, *m*, H(4)), 7.74–7.77 (2H, *m*, H(2) and H(6)). ^{13}C NMR ($CDCl_3$): δ = 25.4 ($N(CH_2)_3\underline{C}H_2$), 26.7 ($N(CH_2)_2\underline{C}H_2$), 29.8 ($NCH_2\underline{C}H_2$), 32.7 ($N(CH_2)_4\underline{C}H_2$), 40.0 ($NCH_2$), 62.8 ($CH_2O$), 127.0 (C(2) and C(6)), 128.7 (C(3) and C(5)), 131.5 (C(4)), 134.9 (C(1)), 167.8 (CO). ESI/MS *m/z* (%): 222 (M^++H, 100), 204 (41).

***N*-(6-Hydroxyhexyl)-3-methoxybenzamide (7).** Procedure A1. η = 88%. ^{1}H NMR ($CDCl_3$): δ = 1.32–1.38 (4H, *m*, $N(CH_2)_2(C\underline{H}_2)_2$), 1.48–1.62 (4H, *m*, $NCH_2C\underline{H}_2(CH_2)_2C\underline{H}_2$), 2.85 (1H, *s*, OH), 3.36–3.41 (2H, *m*, NCH_2), 3.58 (2H, *t*, *J* = 6.5 Hz, CH_2O), 3.79 (3H, *s*, OCH_3), 6.89 (1H, *t*, *J* = 5.4 Hz, NH), 6.99 (1H, *ddd*, *J* = 1.4, 2.4, 7.7 Hz, H(4)), 7.27 (1H, *dd*, *J* = 7.6, 7.7 Hz, H(5)), 7.31 (1H, *ddd*, *J* = 1.4, 1.6, 7.6 Hz, H(6)), 7.36 (1H, *dd*, *J* = 1.6, 2.4 Hz, H(2)). ^{13}C NMR ($CDCl_3$): δ = 25.3 ($N(CH_2)_3\underline{C}H_2$), 26.6 ($N(CH_2)_2\underline{C}H_2$), 29.5 ($NCH_2\underline{C}H_2$), 32.5 ($N(CH_2)_4\underline{C}H_2$), 40.0 ($NCH_2$), 55.4 ($OCH_3$), 62.4 ($CH_2O$), 112.5 (C(4)), 117.4 (C(6)), 118.9 (C(2)), 129.5 (C(5)), 136.2 (C(1)), 159.7 (C(3)), 167.7 (CO). ESI/MS *m/z* (%): 274 (M^++Na, 53), 252 (M^++H, 18), 135 (100).

***N*-(6-Hydroxyhexyl)-4-methoxybenzamide (8).** Procedure A1. η = 69%. ^{1}H NMR ($CDCl_3$): δ = 1.36–1.46 (4H, *m*, $N(CH_2)_2(C\underline{H}_2)_2$), 1.52–1.65 (4H, *m*, $NCH_2C\underline{H}_2(CH_2)_2C\underline{H}_2$), 1.76 (1H, *s*, OH), 3.38–3.49 (2H, *m*, NCH_2), 3.63 (2H, *t*, *J* = 6.4 Hz, CH_2O), 3.83 (3H, *s*, OCH_3), 6.16 (1H, *s*, NH), 6.82–6.99 (2H, *m*, H(3) and H(5)), 7.66–7.81 (2H, *m*, H(2) and H(6)). ^{13}C NMR ($CDCl_3$): δ = 25.4 ($N(CH_2)_3\underline{C}H_2$), 26.7 ($N(CH_2)_2\underline{C}H_2$), 29.9 ($NCH_2\underline{C}H_2$), 32.7 ($N(CH_2)_4\underline{C}H_2$), 39.9 ($NCH_2$), 55.5 ($OCH_3$), 62.8 ($CH_2O$), 113.9 (C(3) and C(5)), 127.2 (C(1)), 128.8 (C(2) and C(6)), 162.2 (C(4)), 167.3 (CO). ESI/MS *m/z* (%): 274 (M^++Na, 48), 252 (M^++H, 14), 135 (100).

***N*-(6-Hydroxyhexyl)-3,4-dimethoxybenzamide (9)** and ***N*-(6-Hydroxyhexyl)-3,4,5-trimethoxybenzamide (12).** Procedure A1. Structural analysis described in literature [39].

***N*-(8-Hydroxyoctyl)-3,4-dimethoxybenzamide (10).** Procedure A2. Structural analysis described in literature [15].

***N*-(10-Hydroxydecyl)-3,4-dimethoxybenzamide (11)**, ***N*-(8-Hydroxyoctyl)-3,4,5-trimethoxybenzamide (13)** and ***N*-(10-Hydroxydecyl)-3,4,5-trimethoxybenzamide (14).** Procedure A2. Structural analysis described in literature [15].

4.1.1.2. General procedure to obtain aldehyde derivatives (15–23). Pyridinium chlorochromate (1.5 mmol) and dichloromethane (20 mL) were added and kept under stirring for 5–7 min. Benzoic acid amide derivative (**6**–**14**) was added and stirred for 2 h. Thereafter diethyl ether (15 mL) was added and the solid was filtrated using a Celite pad. The solvent was evaporated and the compound purified by silica gel flash chromatography using ethyl acetate as eluting system. The control reaction was performed by TLC (silica gel, ethyl acetate). The procedure was adapted from the literature [40].

***N*-(6-Oxohexyl)benzamide (15).** η = 54%. ^{1}H NMR ($CDCl_3$): δ = 1.28–1.40 (2H, *m*, $N(CH_2)_2C\underline{H}_2$), 1.51–1.66 (4H, *m*, $NCH_2C\underline{H}_2CH_2C\underline{H}_2$), 2.39 (2H, *td*, *J* = 1.7, 7.2 Hz, $C\underline{H}_2CHO$), 3.31–3.42 (2H, *m*, NCH_2), 6.74 (1H, *s*, NH), 7.30–7.38 (2H, *m*, H(3) and H(5)), 7.38–7.46 (1H, *m*, H(4)), 7.64–7.88 (2H, *m*, H(2) and H(6)), 9.69 (1H, *t*, *J* = 1.7 Hz, CHO). ^{13}C NMR ($CDCl_3$): δ = 21.6 ($N(CH_2)_2\underline{C}H_2$), 26.4 ($N(CH_2)_3\underline{C}H_2$), 29.3 ($NCH_2\underline{C}H_2$), 39.8 ($NCH_2$), 43.7 ($\underline{C}H_2CHO$), 127.0 (C(2) and C(6)), 128.5 (C(3) and C(5)), 131.4 (C(4)), 134.6 (C(1)), 167.8 (CONH), 202.7 (CHO). ESI/MS *m/z* (%): 220 (M^++H, 7), 105 (100).

3-Methoxy-*N*-(6-oxohexyl)benzamide (16). η = 56%. ^{1}H NMR ($CDCl_3$): δ = 1.28–1.38 (2H, *m*, $N(CH_2)_2C\underline{H}_2$), 1.51–1.64 (4H, *m*, $NCH_2C\underline{H}_2CH_2C\underline{H}_2$), 2.38 (2H, *td*, *J* = 1.6, 7.2 Hz, $C\underline{H}_2CHO$), 3.33–3.41 (2H, *m*, NCH_2), 3.76 (3H, *s*, OCH_3), 6.83 (1H, *s*, NH), 6.96 (1H, *ddd*, *J* = 1.4, 2.6, 7.7 Hz, H(4)), 7.24 (1H, *dd*, *J* = 7.6, 7.7 Hz, H(5)), 7.28 (1H, *ddd*, *J* = 1.4, 1.6, 7.6 Hz, H(6)), 7.33 (1H, *dd*, *J* = 1.6, 2.3 Hz, H(2)), 9.69 (1H, *t*, *J* = 1.6 Hz, CHO). ^{13}C NMR ($CDCl_3$): δ = 21.5 ($N(CH_2)_2\underline{C}H_2$), 26.3 ($N(CH_2)_3\underline{C}H_2$), 29.3 ($NCH_2\underline{C}H_2$), 39.7 ($NCH_2$), 43.6 ($\underline{C}H_2CHO$), 55.3 ($OCH_3$), 112.3 (C(4)), 117.4 (C(6)), 118.8 (C(2)), 129.4 (C(5)), 136.1 (C(1)), 159.7 (C(3)), 167.5 (CONH), 202.7 (CHO). ESI/MS *m/z* (%): 250 (M^++H, 35), 135 (100).

4-Methoxy-*N*-(6-oxohexyl)benzamide (17). η = 43%. ^{1}H NMR ($CDCl_3$): δ = 1.35–1.45 (2H, *m*, $N(CH_2)_2C\underline{H}_2$), 1.57–1.70 (4H, *m*, $NCH_2C\underline{H}_2CH_2C\underline{H}_2$), 2.45 (2H, *td*, *J* = 1.6, 7.2 Hz, $C\underline{H}_2CHO$), 3.35–3.48 (2H, *m*, NCH_2), 3.83 (3H, *s*, OCH_3), 6.19 (1H, *s*, NH), 6.82–6.99 (2H, *m*, H(3) and H(5)), 7.66–7.81 (2H, *m*, H(2) and H(6)), 9.76 (1H, *t*, *J* = 1.6 Hz, CHO). ^{13}C NMR ($CDCl_3$): δ = 21.7 ($N(CH_2)_2\underline{C}H_2$), 26.5 ($N(CH_2)_3\underline{C}H_2$), 29.6 ($NCH_2\underline{C}H_2$), 39.8 ($NCH_2$), 43.8 ($\underline{C}H_2CHO$), 55.5 ($OCH_3$), 113.8 (C(3) and C(5)), 127.1 (C(1)), 128.8 (C(2) and C(6)), 162.2 (C(4)), 167.2 (CONH), 202.6 (CHO). ESI/MS *m/z* (%): 250 (M^++H, 12), 135 (100).

3,4-Dimethoxy-*N*-(6-oxohexyl)benzamide (18). η = 45%. ^{1}H NMR ($CDCl_3$): δ = 1.34–1.46 (2H, *m*, $N(CH_2)_2C\underline{H}_2$), 1.54–1.73 (4H, *m*, $NCH_2C\underline{H}_2CH_2C\underline{H}_2$), 2.44 (2H, *td*, *J* = 1.6, 7.2 Hz, $C\underline{H}_2CHO$), 3.38–3.48 (2H, *m*, NCH_2), 3.90 (6H, *s*, 2 × OCH_3), 6.29 (1H, *s*, NH), 6.83 (1H, *d*, *J* = 8.4 Hz, H(5)), 7.27 (1H, *dd*, *J* = 2.0, 8.4 Hz, H(6)), 7.41 (1H, *d*, *J* = 2.0 Hz, H(2)), 9.75 (1H, *t*, *J* = 1.6 Hz, CHO). ^{13}C NMR ($CDCl_3$): δ = 21.6 ($N(CH_2)_2\underline{C}H_2$), 26.5 ($N(CH_2)_3\underline{C}H_2$), 29.5 ($NCH_2\underline{C}H_2$), 39.8 ($NCH_2$), 43.8 ($\underline{C}H_2CHO$), 56.1 (2 × OCH_3), 110.4 (C(5)), 110.7 (C(2)), 119.3 (C(6)), 127.5 (C(1)), 149.1 (C(3)), 151.8 (C(4)), 167.2 (CONH), 202.6 (CHO). EI/MS *m/z* (%): 279 (M^+, 41), 251 (87), 250 (26), 236 (72), 222 (28), 195 (58), 194 (40), 182 (22), 181 (90), 166 (82), 165 (100), 137 (32), 122 (26), 92 (20), 79 (35), 77 (42).

3,4-Dimethoxy-*N*-(8-oxooctyl)benzamide (19). η = 66%. ^{1}H NMR ($CDCl_3$): δ = 1.22–1.44 (6H, *m*, $N(CH_2)_2(C\underline{H}_2)_3$), 1.54–1.68 (4H, *m*, $NCH_2C\underline{H}_2(CH_2)_3C\underline{H}_2$), 2.41 (2H, *td*, *J* = 1.8, 7.3 Hz, $C\underline{H}_2CHO$), 3.34–3.46 (2H, *m*, NCH_2), 3.90 (6H, *s*, 2 × OCH_3), 6.17 (1H, *s*, NH), 6.84 (1H, *d*, *J* = 8.4 Hz, H(5)), 7.25 (1H, *dd*, *J* = 2.0, 8.4 Hz, H(6)), 7.41 (1H, *d*, *J* = 2.0 Hz, H(2)), 9.75 (1H, *t*, *J* = 1.8 Hz, CHO). ^{13}C NMR ($CDCl_3$): δ = 22.0 ($N(CH_2)_2\underline{C}H_2$), 26.9 ($N(CH_2)_5\underline{C}H_2$), 29.1 ($N(CH_2)_3(\underline{C}H_2)_2$), 29.8 ($NCH_2\underline{C}H_2$), 40.1 ($NCH_2$), 43.9 ($\underline{C}H_2CHO$), 56.1 (2 × OCH_3), 110.4 (C(5)), 110.8 (C(2)), 119.2 (C(6)), 127.6 (C(1)), 149.1 (C(3)), 151.7 (C(4)), 167.2 (CONH), 202.9 (CHO). ESI/MS *m/z* (%): 308 (M^++H, 100), 165 (60), 124 (23).

3,4-Dimethoxy-*N*-(10-oxodecyl)benzamide (20). η = 71%. ^{1}H NMR ($CDCl_3$): δ = 1.23–1.37 (10H, *m*, $N(CH_2)_2(C\underline{H}_2)_5$), 1.51–1.64 (4H, *m*, $NCH_2C\underline{H}_2(CH_2)_5C\underline{H}_2$), 2.40 (2H, *td*, *J* = 1.8, 7.3 Hz, $C\underline{H}_2CHO$), 3.37–3.44 (2H, *m*, NCH_2), 3.90 (6H, *s*, 2 × OCH_3), 6.20 (1H, *s*, NH), 6.83 (1H, *d*, *J* = 8.4 Hz, H(5)), 7.25 (1H, *dd*, *J* = 2.0, 8.4 Hz, H(6)), 7.41 (1H, *d*, *J* = 2.0 Hz, H(2)), 9.74 (1H, *t*, *J* = 1.8 Hz, CHO). ^{13}C NMR ($CDCl_3$): δ = 22.1 ($N(CH_2)_2\underline{C}H_2$), 27.0 ($N(CH_2)_7\underline{C}H_2$), 29.2 ($N(CH_2)_3\underline{C}H_2$), 29.3 ($N(CH_2)_6\underline{C}H_2$), 29.4 ($N(CH_2)_4(\underline{C}H_2)_2$), 29.8 ($NCH_2\underline{C}H_2$), 40.2 ($NCH_2$), 44.0 ($\underline{C}H_2CHO$), 56.1 (2 × OCH_3), 110.4 (C(5)), 110.8 (C(2)), 119.2 (C(6)), 127.6 (C(1)), 149.1 (C(3)), 151.7 (C(4)), 167.2 (CONH), 203.0 (CHO).

3,4,5-Trimethoxy-*N*-(6-oxohexyl)benzamide (21). η = 50%. ^{1}H NMR ($CDCl_3$): δ = 1.35–1.45 (2H, *m*, $N(CH_2)_2C\underline{H}_2$), 1.57–1.72 (4H, *m*, $NCH_2C\underline{H}_2CH_2C\underline{H}_2$), 2.46 (2H, *td*, *J* = 1.6, 7.1 Hz, $C\underline{H}_2CHO$), 3.41–3,49 (2H, *m*, NCH_2), 3.86 (3H, *s*, OCH_3), 3.88 (6H, *s*, 2 × OCH_3), 6.32 (1H, *s*, NH), 7.00 (2H, *s*, H(2) and H(6)), 9.76 (1H, *t*, *J* = 1.6 Hz, CHO). ^{13}C NMR ($CDCl_3$): δ = 21.5 ($N(CH_2)_2\underline{C}H_2$), 26.4 ($N(CH_2)_3\underline{C}H_2$), 29.4 ($NCH_2\underline{C}H_2$), 39.9 ($NCH_2$), 43.8 ($\underline{C}H_2CHO$), 56.4 (2 × OCH_3), 61.0 (OCH_3), 104.5 (C(2) and C(6)), 130.2 (C(1)), 141.0 (C(4)), 153.3 (C(3) and C(5)), 167.4 (CONH), 202.6 (CHO). EI/MS *m/z* (%): 309 (M^+, 92), 281 (35), 280 (21), 266 (59), 225 (37), 224 (27), 211 (89), 196 (96), 195 (100), 154 (20), 152 (29), 137 (26), 109 (20), 81 (25).

3,4,5-Trimethoxy-*N*-(8-oxooctyl)benzamide (22). η = 63%. ^{1}H NMR ($CDCl_3$): δ = 1.27–1.45 (6H, *m*, $N(CH_2)_2(C\underline{H}_2)_3$), 1.54–1.71 (4H, *m*, $NCH_2C\underline{H}_2(CH_2)_3C\underline{H}_2$), 2.43 (2H, *t*, *J* = 6.8 Hz, $C\underline{H}_2CHO$), 3.36–3.48 (2H, *m*, NCH_2), 3.87 (3H, *s*, OCH_3), 3.90 (6H, *s*, 2 × OCH_3), 6.08 (1H, *s*, CONH), 6.98 (2H, *s*, H(2) and H(6)), 9.76 (1H, *s*, CHO). ^{13}C NMR ($CDCl_3$): δ = 22.0 ($N(CH_2)_2\underline{C}H_2$), 26.9 ($N(CH_2)_5\underline{C}H_2$), 29.1 ($N(CH_2)_3(\underline{C}H_2)_2$), 29.8 ($NCH_2\underline{C}H_2$), 40.3 ($NCH_2$), 44.0 ($\underline{C}H_2CHO$), 56.5 (2 × OCH_3), 61.0 (OCH_3), 104.5 (C(2) and C(6)), 130.5 (C(1)), 141.0 (C(4)), 153.3 (C(3) and C(5)), 167.4 (CONH), 202.9 (CHO). ESI/MS *m/z* (%): 360 (M^++Na, 20), 338 (M^++H, 100), 195 (88), 169 (24), 154 (78).

3,4,5-Trimethoxy-*N*-(10-oxodecyl)benzamide (23). η = 77%. ^{1}H NMR ($CDCl_3$): δ = 1.23–1.43 (10H, *m*, $N(CH_2)_2(C\underline{H}_2)_5$), 1.52–1.71 (4H, *m*, $NCH_2C\underline{H}_2(CH_2)_5C\underline{H}_2$), 2.46 (2H, *t*, *J* = 7.2 Hz, $C\underline{H}_2CHO$), 3.38–3.47 (2H, *m*, NCH_2), 3.87 (3H, *s*, OCH_3), 3.90 (6H, *s*, 2 × OCH_3), 6.09 (1H, *s*, NH), 6.98 (2H, *s*, H(2) and H(6)), 9.75 (1H, *s*, CHO). ^{13}C NMR ($CDCl_3$): δ = 22.2 ($N(CH_2)_2\underline{C}H_2$), 27.1 ($N(CH_2)_7\underline{C}H_2$), 29.2 ($N(CH_2)_3\underline{C}H_2$), 29.3 ($N(CH_2)_6\underline{C}H_2$), 29.4 ($N(CH_2)_4(\underline{C}H_2)_2$), 29.9 ($NCH_2\underline{C}H_2$), 40.4 ($NCH_2$), 44.0 ($\underline{C}H_2CHO$), 56.5 (2 × OCH_3), 61.0 (OCH_3), 104.5 (C(2) and C(6)), 130.5 (C(1)), 141.0 (C(4)), 153.3 (C(3) and C(5)), 167.3 (CONH), 203.0 (CHO). ESI/MS *m/z* (%): 366 (M^++H, 100), 195 (33), 154 (35).

4.1.1.3. General procedure to obtain nitrone derivatives (24–42). In a microwave vial the aldehyde derivative (**15**–**23**, 1 mmol), hydroxylamine hydrochloride (*N-tert*-butyl, *N*-benzyl or *N*-cyclohexyl, 1.5 mmol) and $NaHCO_3$ (1.5 mmol) were added in 3–5 mL of tetrahydrofuran at 90 °C for 10 min with 10 s of pre-stirring. Dichloromethane (20 mL) was added and extracted with water (2 × 10 mL). The organic phases were combined, the solvent was evaporated and the compound purified by silica gel flash chromatography using ethyl acetate:methanol (9:1) as eluting system. The control reaction was performed by TLC (silica gel, ethyl acetate).

α-5-Benzamidopentyl-*N*-*tert*-butyl nitrone (24). η = 51%. ^{1}H NMR (CD_3OD): δ = 1.38–1.53 (11H, *m*, $C(C\underline{H}_3)_3$ and $N(CH_2)_3C\underline{H}_2$), 1.57–1.73 (4H, *m*, $N(CH_2)_2C\underline{H}_2CH_2C\underline{H}_2$), 2.39–2.58 (2H, *m*, $NCH_2C\underline{H}_2$), 3.40 (2H, *t*, *J* = 7.0, NCH_2), 7.25 (1H, *t*, *J* = 5.7 Hz, CH=N^+), 7.41–7.48 (2H, *m*, H(3) and H(5)), 7.49–7.55 (1H, *m*, H(4)), 7.77–7.85 (2H, *m*, H(2) and H(6)). ^{13}C NMR (CD_3OD): δ = 26.1 ($N(CH_2)_2\underline{C}H_2$), 27.9 ($N(CH_2)_3\underline{C}H_2$), 28.0 ($C(\underline{C}H_3)_3$), 28.2 ($NCH_2\underline{C}H_2$), 30.1 ($N(CH_2)_4\underline{C}H_2$), 40.7 ($NCH_2$), 70.5 ($\underline{C}(CH_3)_3$), 128.2 (C(2) and C(6)), 129.5 (C(3) and C(5)), 132.5 (C(4)), 135.8 (C(1)), 142.2 (CH=N^+), 170.2 (CO). ESI/MS *m/z* (%): 313 (M^++Na, 26), 291 (M^++H, 7), 290 (M^+, 5), 105 (100). ESI/HRMS calcd for $C_{17}H_{26}N_2O_2$ (M^+): 290.1994, found 290.1966.

α-5-Benzamidopentyl-*N*-benzyl nitrone (25). η = 31%. ^{1}H NMR (CD_3OD): δ = 1.38–1.53 (2H, *m*, $N(CH_2)_3C\underline{H}_2$), 1.57–1.72 (4H, *m*, $N(CH_2)_2C\underline{H}_2CH_2C\underline{H}_2$), 2.44–2.53 (2H, *m*, $NCH_2C\underline{H}_2$), 3.38 (2H, *t*, *J* = 7.0 Hz, NCH_2), 4.93 (2H, *s*, N^+CH_2), 7.31–7.48 (8H, *m*, H(2′–6′), H(3) and H(5) and CH=N^+), 7.49–7.56 (1H, *m*, H(4)), 7.78–7.84 (2H, *m*, H(2) and H(6)). ^{13}C NMR (CD_3OD): δ = 26.0 ($N(CH_2)_2\underline{C}H_2$), 27.8 ($N(CH_2)_3(\underline{C}H_2)_2$), 30.1 ($NCH_2\underline{C}H_2$), 40.7 ($NCH_2$), 69.4 ($N^+CH_2$), 128.2 (C(2) and C(6)), 129.5 (C(3) and C(5)), 129.8 (C(2′) and C(6′)), 130.0 (C(4′)), 130.1 (C(3′) and C(5′)), 132.6 (C(4)), 134.7 (C(1′)), 135.9 (C(1)), 146.3 (CH=N^+), 170.2 (CO). ESI/MS *m/z* (%): 348 (M^++Na+H, 22), 347 (M^++Na, 87), 325 (M^++H, 100), 105 (60), 91 (22). ESI/

HRMS calcd for $C_{20}H_{25}N_2O_2$ (M^++H): 325.1911, found 325.1906.

α-5-Benzamidopentyl-*N*-cyclohexyl nitrone (26). η = 58%. ^{1}H NMR (CD_3OD): δ = 1.20–1.94 (16H, *m*, $N(CH_2)_2(CH_2)_3$ and $N^+CH(CH_2)_5$), 2.41–2.52 (2H, *m*, NCH_2CH_2), 3.39 (2H, *t*, *J* = 7.0 Hz, NCH_2), 3.74–3.86 (1H, *m*, N^+CH), 7.21 (1H, *t*, *J* = 5.9 Hz, $CH{=}N^+$), 7.41–7.48 (2H, *m*, H(3) and H(5)), 7.49–7.56 (1H, *m*, H(4)), 7.76–7.85 (2H, *m*, H(2) and H(6)). ^{13}C NMR (CD_3OD): δ = 25.9 ($N^+CHCH_2CH_2CH_2CH_2$), 26.1 ($N^+CH(CH_2)_2CH_2$ and $N(CH_2)_2CH_2$), 27.5 ($N(CH_2)_3CH_2$), 27.7 (NCH_2CH_2), 30.1 ($N(CH_2)_4CH_2$), 31.9 ($N^+CHCH_2(CH_2)_3CH_2$), 40.7 (NCH_2), 74.5 (N^+CH), 128.2 (C(2) and C(6)), 129.5 (C(3) and C(5)), 132.5 (C(4)), 135.9 (C(1)), 144.2 ($CH{=}N^+$), 170.2 (CO). ESI/MS *m/z* (%): 339 (M^++Na, 94), 317 (M^++H, 100). ESI/HRMS calcd for $C_{19}H_{29}N_2O_2$ (M^++H): 317.2224, found 317.2222.

α-5-(3-Methoxybenzamido)pentyl-*N*-*tert*-butyl nitrone (27). η = 83%. ^{1}H NMR (CD_3OD): δ = 1.43–1.49 (11H, *m*, $C(CH_3)_3$ and $N(CH_2)_3CH_2$), 1.58–1.71 (4H, *m*, $N(CH_2)_2CH_2CH_2CH_2$), 2.45–2.52 (2H, *m*, NCH_2CH_2), 3.39 (2H, *t*, *J* = 7.0 Hz, NCH_2), 3.84 (3H, *s*, OCH_3), 7.06–7.10 (1H, *m*, H(2)), 7.25 (1H, *t*, *J* = 5.7 Hz, $CH{=}N^+$), 7.32–7.40 (3H, *m*, H(4–6)). ^{13}C NMR (CD_3OD): δ = 26.1 ($N(CH_2)_2CH_2$), 27.9 ($N(CH_2)_3CH_2$), 28.0 ($C(CH_3)_3$), 28.2 (NCH_2CH_2), 30.1 ($N(CH_2)_4CH_2$), 40.7 (NCH_2), 55.9 (OCH_3), 70.5 ($C(CH_3)_3$), 113.6 (C(4)), 118.3 (C(6)), 120.3 (C(2)), 130.6 (C(5)), 137.2 (C(1)), 142.2 ($CH{=}N^+$), 161.3 (C(3)), 170.0 (CO). ESI/MS *m/z* (%): 321 (M^++H, 8), 135 (100). ESI/HRMS calcd for $C_{19}H_{29}N_2O_3$ (M^++H): 321.2173, found 321.2163.

α-5-(3-Methoxybenzamido)pentyl-*N*-benzyl nitrone (28). η = 38%. ^{1}H NMR (CD_3OD): δ = 1.39–1.49 (2H, *m*, $N(CH_2)_3CH_2$), 1.56–1.69 (4H, *m*, $N(CH_2)_2CH_2CH_2CH_2$), 2.43–2.52 (2H, *m*, NCH_2CH_2), 3.37 (2H, *t*, *J* = 7.0 Hz, NCH_2), 3.83 (3H, *s*, OCH_3), 4.92 (2H, *s*, N^+CH_2), 7.05–7.10 (1H, *m*, H(2)), 7.31–7.45 (9H, *m*, H(2′–6′), H(4–6) and $CH{=}N^+$). ^{13}C NMR (100 MHz, CD_3OD): δ = 26.0 ($N(CH_2)_2CH_2$), 27.7 ($N(CH_2)_3CH_2$), 27.8 ($N(CH_2)_4CH_2$), 30.1 (NCH_2CH_2), 40.7 (NCH_2), 55.9 (OCH_3), 69.4 (N^+CH_2), 113.6 (C(4)), 118.3 (C(6)), 120.3 (C(2)), 129.8 (C(2′) and C(6′)), 129.9 (C(4′)), 130.1 (C(3′) and C(5′)), 130.6 (C(5)), 134.7 (C(1′)), 137.2 (C(1)), 146.2 ($CH{=}N^+$), 161.3 (C(3)), 170.0 (CO). ESI/MS *m/z* (%): 377 (M^++Na, 58), 355 (M^++H, 100), 135 (84), 91 (25). ESI/HRMS calcd for $C_{21}H_{27}N_2O_3$ (M^++H): 355.2016, found 355.2046.

α-5-(3-Methoxybenzamido)pentyl-*N*-cyclohexyl nitrone (29). η = 78%. ^{1}H NMR (CD_3OD): δ = 1.20–1.93 (16H, *m*, $N(CH_2)_2(CH_2)_3$ and $N^+CH(CH_2)_5$), 2.42–2.52 (2H, *m*, NCH_2CH_2), 3.39 (2H, *t*, *J* = 7.0 Hz, NCH_2), 3.74–3.83 (1H, *m*, N^+CH), 3.84 (3H, *s*, OCH_3), 7.06–7.10 (1H, *m*, H(2)), 7.20 (1H, *t*, *J* = 5.9 Hz, $CH{=}N^+$), 7.32–7.40 (3H, *m*, H(4–6)). ^{13}C NMR (CD_3OD): δ = 25.9 ($N^+CHCH_2CH_2CH_2CH_2$), 26.1 ($N^+CH(CH_2)_2CH_2$ and $N(CH_2)_2CH_2$), 27.5 ($N(CH_2)_3CH_2$), 27.7 (NCH_2CH_2), 30.1 ($N(CH_2)_4CH_2$), 31.9 ($N^+CHCH_2(CH_2)_3CH_2$), 40.7 (NCH_2), 55.9 (OCH_3), 74.6 (N^+CH), 113.7 (C(4)), 118.3 (C(6)), 120.3 (C(2)), 130.6 (C(5)), 137.2 (C(1)), 144.2 ($CH{=}N^+$), 161.3 (C(3)), 170.0 (CO). ESI/MS *m/z* (%): 369 (M^++Na, 62), 347 (M^++H, 48), 135 (100). ESI/HRMS calcd for $C_{20}H_{31}N_2O_3$ (M^++H): 347.2329, found 347.2324.

α-5-(4-Methoxybenzamido)pentyl-*N*-*tert*-butyl nitrone (30). η = 62%. ^{1}H NMR (CD_3OD): δ = 1.39–1.51 (11H, *m*, $C(CH_3)_3$ and $N(CH_2)_3CH_2$), 1.56–1.71 (4H, *m*, $N(CH_2)_2CH_2CH_2CH_2$), 2.42–2.53 (2H, *m*, NCH_2CH_2), 3.38 (2H, *t*, *J* = 7.0 Hz, NCH_2), 3.84 (3H, *s*, OCH_3), 6.93–7.01 (2H, *m*, H(3) and H(5)), 7.25 (1H, *t*, *J* = 5.7 Hz, $CH{=}N^+$), 7.76–7.81 (2H, *m*, H(2) and H(6)). ^{13}C NMR (CD_3OD): δ = 26.1 ($N(CH_2)_2CH_2$), 27.9 ($N(CH_2)_3CH_2$), 28.0 ($C(CH_3)_3$), 28.2 (NCH_2CH_2), 30.2 ($N(CH_2)_4CH_2$), 40.6 (NCH_2), 55.9 (OCH_3), 70.5 ($C(CH_3)_3$), 114.7 (C(3) and C(5)), 127.9 (C(1)), 130.1 (C(2) and C(6)), 142.2 ($CH{=}N^+$), 163.8 (C(4)), 169.8 (CO). ESI/MS *m/z* (%): 343 (M^++Na, 16), 321 (M^++H, 4), 135 (100). ESI/HRMS calcd for $C_{18}H_{29}N_2O_3$ (M^++H): 321.2173, found 321.2172.

α-5-(4-Methoxybenzamido)pentyl-*N*-benzyl nitrone (31). η = 31%. ^{1}H NMR (CD_3OD): δ = 1.37–1.49 (2H, *m*, $N(CH_2)_3CH_2$), 1.56–1.69 (4H, *m*, $N(CH_2)_2CH_2CH_2CH_2$), 2.43–2.53 (2H, *m*, NCH_2CH_2), 3.36 (2H, *t*, *J* = 7.0 Hz, NCH_2), 3.83 (3H, *s*, OCH_3), 4.93 (2H, *s*, N^+CH_2), 6.92–7.03 (2H, *m*, H(3) and H(5)), 7.30–7.46 (6H, *m*, H(2′–6′) and $CH{=}N^+$), 7.73–7.83 (2H, *m*, H(2) and H(6)). ^{13}C NMR (CD_3OD): δ = 26.0 ($N(CH_2)_2CH_2$), 27.8 ($N(CH_2)_3(CH_2)_2$), 30.2 (NCH_2CH_2), 40.6 (NCH_2), 55.9 (OCH_3), 69.4 (N^+CH_2), 114.7 (C(3) and C(5)), 127.9 (C(1)), 129.8 (C(2′) and C(6′)), 129.9 (C(4′)), 130.1 (C(2), C(6), C(3′) and C(5′)), 134.7 (C(1′)), 146.2 ($CH{=}N^+$), 163.9 (C(4)), 169.8 (CO). ESI/MS *m/z* (%): 378 (M^++Na+H, 24), 377 (M^++Na, 100), 286 (26), 228 (32). ESI/HRMS calcd for $C_{21}H_{26}N_2O_3Na$ (M^++Na): 377.1836, found 377.1840.

α-5-(4-Methoxybenzamido)pentyl-*N*-cyclohexyl nitrone (32). η = 39%. ^{1}H NMR (CD_3OD): δ = 1.19–1.92 (16H, *m*, $N(CH_2)_2(CH_2)_3$ and $N^+CH(CH_2)_5$), 2.41–2.51 (2H, *m*, NCH_2CH_2), 3.37 (2H, *t*, *J* = 7.0 Hz, NCH_2), 3.74–3.83 (1H, *m*, N^+CH), 3.84 (3H, *s*, OCH_3), 6.93–7.00 (2H, *m*, H(3) and H(5)), 7.20 (1H, *t*, *J* = 5.9 Hz, $CH{=}N^+$), 7.75–7.82 (2H, *m*, H(2) and H(6)). ^{13}C NMR (CD_3OD): δ = 25.9 ($N^+CHCH_2CH_2CH_2CH_2$), 26.1 ($N^+CH(CH_2)_2CH_2$ and $N(CH_2)_2CH_2$), 27.5 ($N(CH_2)_3CH_2$), 27.7 (NCH_2CH_2), 30.2 ($N(CH_2)_4CH_2$), 31.9 ($N^+CHCH_2(CH_2)_3CH_2$), 40.6 (NCH_2), 55.9 (OCH_3), 74.5 (N^+CH), 114.7 (C(3) and C(5)), 127.9 (C(1)), 130.1 (C(2) and C(6)), 144.2 ($CH{=}N^+$), 163.8 (C(4)), 169.8 (CO). ESI/MS *m/z* (%): 369 (M^++Na, 17), 135 (100). ESI/HRMS calcd for $C_{20}H_{30}N_2O_3Na$ (M^++Na): 369.2149, found 369.2146.

α-5-(3,4-Dimethoxybenzamido)pentyl-*N*-*tert*-butyl nitrone (33). η = 90%. ^{1}H NMR (CD_3OD): δ = 1.40–1.49 (11H, *m*, $C(CH_3)_3$ and $N(CH_2)_3CH_2$), 1.58–1.71 (4H, *m*, $N(CH_2)_2CH_2CH_2CH_2$), 2.43–2.52 (2H, *m*, NCH_2CH_2), 3.38 (2H, *t*, *J* = 7.0 Hz, NCH_2), 3.88 (6H, *s*, 2 × OCH_3), 7.00 (1H, *d*, *J* = 8.4 Hz, H(5)), 7.25 (1H, *t*, *J* = 5.7 Hz, $CH{=}N^+$), 7.42–7.49 (2H, *m*, H(2) and H(6)). ^{13}C NMR (CD_3OD): δ = 26.1 ($N(CH_2)_2CH_2$), 27.9 ($N(CH_2)_3CH_2$), 28.0 ($C(CH_3)_3$), 28.2 (NCH_2CH_2), 30.2 ($N(CH_2)_4CH_2$), 40.7 (NCH_2), 56.5 (2 × OCH_3), 70.5 ($C(CH_3)_3$), 112.0 (C(5) and C(2)), 121.8 (C(6)), 128.2 (C(1)), 142.2 ($CH{=}N^+$), 150.3 (C(3)), 153.4 (C(4)), 169.7 (CO). ESI/MS *m/z* (%): 373 (M^++Na, 16), 373 (M^++H, 8), 165 (100). ESI/HRMS calcd for $C_{19}H_{31}N_2O_4$ (M^++H): 351.2278, found 351.2260.

α-5-(3,4-Dimethoxybenzamido)pentyl-*N*-benzyl nitrone (34). η = 43%. ^{1}H NMR (CD_3OD): δ = 1.39–1.49 (2H, *m*, $N(CH_2)_3CH_2$), 1.55–1.69 (4H, *m*, $N(CH_2)_2CH_2CH_2CH_2$), 2.43–2.53 (2H, *m*, NCH_2CH_2), 3.37 (2H, *t*, *J* = 7.0 Hz, NCH_2), 3.87 (6H, *s*, 2 × OCH_3), 4.93 (2H, *s*, N^+CH_2), 7.00 (1H, *d*, *J* = 8.2 Hz, H(5)), 7.31–7.48 (8H, *m*, H(2′–6′), $CH{=}N^+$, H(2) and H(6)). ^{13}C NMR (CD_3OD): δ = 26.0 ($N(CH_2)_2CH_2$), 27.8 ($N(CH_2)_3(CH_2)_2$), 30.2 (NCH_2CH_2), 40.7 (NCH_2), 56.5 (2 × OCH_3), 69.4 (N^+CH_2), 112.0 (C(5) and C(2)), 121.8 (C(6)), 128.2 (C(1)), 129.8 (C(2′) and C(6′)), 129.9 (C(4′)), 130.1 (C(3′) and C(5′)), 134.7 (C(1′)), 146.2 ($CH{=}N^+$), 150.3 (C(3)), 153.4 (C(4)), 169.7 (CO). ESI/MS *m/z* (%): 407 (M^++Na, 28), 385 (M^++H, 95), 165 (100). ESI/HRMS calcd for $C_{22}H_{29}N_2O_4$ (M^++H): 385.2122, found 385.2121.

α-5-(3,4-Dimethoxybenzamido)pentyl-*N*-cyclohexyl nitrone (35). η = 57%. ^{1}H NMR (CD_3OD): δ = 1.19–1.91 (16H, *m*, $N(CH_2)_2(CH_2)_3$ and $N^+CH(CH_2)_5$), 2.40–2.59 (2H, *m*, NCH_2CH_2), 3.38 (2H, *t*, *J* = 7.0 Hz, NCH_2), 3.72–3.84 (1H, *m*, N^+CH), 3.88 (6H, *s*, 2 × OCH_3), 7.00 (1H, *d*, *J* = 8.3 Hz, H(5)), 7.19 (1H, *t*, *J* = 5.7 Hz, $CH{=}N^+$), 7.40–7.49 (2H, *m*, H(2) and H(6)). ^{13}C NMR (CD_3OD): δ = 25.9 ($N^+CHCH_2CH_2CH_2CH_2$), 26.1 ($N^+CH(CH_2)_2CH_2$ and $N(CH_2)_2CH_2$), 27.5 ($N(CH_2)_3CH_2$), 27.7 (NCH_2CH_2), 30.2 ($N(CH_2)_4CH_2$), 31.9 ($N^+CHCH_2(CH_2)_3CH_2$), 40.7 (NCH_2), 56.5 (2 × OCH_3), 74.6 (N^+CH), 112.0 (C(5) and C(2)), 121.8 (C(6)), 128.2 (C(1)), 144.2 ($CH{=}N^+$), 150.3 (C(3)), 153.4 (C(4)), 169.7 (CO). ESI/MS *m/z* (%): 399 (M^++Na, 40), 377 (M^++H, 24), 165 (100). ESI/HRMS calcd for $C_{21}H_{33}N_2O_4$ (M^++H): 377.2435, found 377.2426.

α-7-(3,4-Dimethoxybenzamido)heptyl-*N*-*tert*-butyl nitrone (36). η = 71%. ^{1}H NMR (CD_3OD): δ = 1.37–1.43 (6H, *m*, $N(CH_2)_2(CH_2)_2CH_2CH_2$), 1.47 (9H, *s*, $C(CH_3)_3$), 1.53–1.65 (4H, *m*, $N(CH_2)_4CH_2CH_2CH_2$), 2.40–2.49 (2H, *m*, NCH_2CH_2), 3.36 (2H, *t*, *J* = 7.2 Hz, NCH_2), 3.87 (6H, *s*, 2 × OCH_3), 7.00 (1H, *d*, *J* = 8.5 Hz,

H(5)), 7.24 (1H, *t*, *J* = 5.7 Hz, CH=N$^+$), 7.42–7.47 (2H, *m*, H(2) and H(6)). ^{13}C NMR (CD_3OD): δ = 26.3 ($N(CH_2)_2\underline{C}H_2$), 27.9 ($N(CH_2)_5\underline{C}H_2$), 28.0 ($C(\underline{C}H_3)_3$), 28.3 ($N(CH_2)_3\underline{C}H_2$), 30.1 ($N(CH_2)_4\underline{C}H_2$), 30.5 ($NCH_2\underline{C}H_2$), 30.6 ($N(CH_2)_6\underline{C}H_2$), 41.0 ($NCH_2$), 56.5 (2 × OCH_3), 70.5 ($\underline{C}(CH_3)_3$), 112.0 (C(5) and C(2)), 121.7 (C(6)), 128.2 (C(1)), 142.4 (CH=N$^+$), 150.2 (C(3)), 153.4 (C(4)), 169.7 (CO). ESI/MS *m/z* (%): 401 (M$^+$+Na, 3), 379 (M$^+$+H, 1), 308 (58), 165 (100), 124 (28). ESI/HRMS calcd for $C_{21}H_{35}N_2O_4$ (M$^+$+H): 379.2591, found 379.2577.

α-9-(3,4-Dimethoxybenzamido)nonyl-*N*-*tert*-butyl nitrone (37). η = 82%. ^{1}H NMR (CD_3OD): δ = 1.31–1.42 (10H, *m*, $N(CH_2)_2(\underline{C}H_2)_4CH_2\underline{C}H_2$), 1.47 (9H, *s*, $C(\underline{C}H_3)_3$), 1.53–1.64 (4H, *m*, $N(CH_2)_6\underline{C}H_2CH_2\underline{C}H_2$), 2.40–2.49 (2H, *m*, $NCH_2\underline{C}H_2$), 3.35 (2H, *t*, *J* = 7.2 Hz, NCH_2), 3.87 (6H, *s*, 2 × OCH_3), 7.00 (1H, *d*, *J* = 8.6 Hz, H(5)), 7.24 (1H, *t*, *J* = 5.7 Hz, CH=N$^+$), 7.41–7.47 (2H, *m*, H(2) and H(6)). ^{13}C NMR (CD_3OD): δ = 26.4 ($N(CH_2)_2\underline{C}H_2$), 28.0 ($C(\underline{C}H_3)_3$), 28.1 ($N(CH_2)_7\underline{C}H_2$), 28.3 ($N(CH_2)_3\underline{C}H_2$), 30.3 ($N(CH_2)_6\underline{C}H_2$), 30.4 ($N(CH_2)_4\underline{C}H_2$), 30.5 ($N(CH_2)_5\underline{C}H_2$), 30.6 ($NCH_2\underline{C}H_2(CH_2)_6\underline{C}H_2$), 41.0 ($NCH_2$), 56.5 (2 × OCH_3), 70.5 ($\underline{C}(CH_3)_3$), 111.9 (C(5)), 112.0 (C(2)), 121.7 (C(6)), 128.3 (C(1)), 142.4 (CH=N$^+$), 150.2 (C(3)), 153.4 (C(4)), 169.7 (CO). ESI/MS *m/z* (%): 406 (M$^+$+Na, 3), 165 (100), 139 (27), 124 (47). ESI/HRMS calcd for $C_{23}H_{38}N_2O_4Na$ (M$^+$+Na): 429.2724, found 429.2716.

α-5-(3,4,5-Trimethoxybenzamido)pentyl-*N*-*tert*-butyl nitrone (38). η = 94%. ^{1}H NMR (CD_3OD): δ = 1.40–1.50 (11H, *m*, $C(CH_3)_3$ and $N(CH_2)_3\underline{C}H_2$), 1.59–1.71 (4H, *m*, $N(CH_2)_2\underline{C}H_2CH_2\underline{C}H_2$), 2.44–2.52 (2H, *m*, $NCH_2\underline{C}H_2$), 3.39 (2H, *t*, *J* = 7.0 Hz, NCH_2), 3.80 (3H, *s*, OCH_3), 3.89 (6H, *s*, 2 × OCH_3), 7.17 (2H, *s*, H(2) and H(6)), 7.25 (1H, *t*, *J* = 5.7 Hz, CH=N$^+$). ^{13}C NMR (CD_3OD): δ = 26.1 ($N(CH_2)_2\underline{C}H_2$), 27.9 ($N(CH_2)_3\underline{C}H_2$), 28.0 ($C(\underline{C}H_3)_3$), 28.2 ($NCH_2\underline{C}H_2$), 30.2 ($N(CH_2)_4\underline{C}H_2$), 40.8 ($NCH_2$), 56.7 (2 × OCH_3), 61.1 (OCH_3), 70.5 ($\underline{C}(CH_3)_3$), 106.0 (C(2) and C(6)), 131.1 (C(1)), 142.1 (C(4)), 142.2 (CH=N$^+$), 154.4 (C(3) and C(5)), 169.5 (CO). EI/MS *m/z* (%): 380 (M$^+$, 37), 307 (20), 266 (31), 212 (45), 196 (51), 195 (100), 96 (34).

α-5-(3,4,5-Trimethoxybenzamido)pentyl-*N*-benzyl nitrone (39). η = 41%. ^{1}H NMR (CD_3OD): δ = 1.39–1.48 (2H, *m*, $N(CH_2)_3\underline{C}H_2$), 1.58–1.69 (4H, *m*, $N(CH_2)_2\underline{C}H_2CH_2\underline{C}H_2$), 2.45–2.53 (2H, *m*, $NCH_2\underline{C}H_2$), 3.37 (2H, *t*, *J* = 7.0 Hz, NCH_2), 3.80 (3H, *s*, OCH_3), 3.88 (6H, *s*, 2 × OCH_3), 4.92 (2H, *s*, N^+CH_2), 7.17 (2H, *s*, H(2) and H(6)), 7.32–7.44 (6H, *m*, H(2′–6′) and CH=N$^+$). ^{13}C NMR (CD_3OD): δ = 26.0 ($N(CH_2)_2\underline{C}H_2$), 27.7 ($N(CH_2)_3\underline{C}H_2$), 27.8 ($N(CH_2)_4\underline{C}H_2$), 30.1 ($NCH_2\underline{C}H_2$), 40.8 ($NCH_2$), 56.7 (2 × OCH_3), 61.1 (OCH_3), 69.4 ($N^+\underline{C}H_2$), 106.0 (C(2) and C(6)), 129.8 (C(2′) and C(6′)), 129.9 (C(4′)), 130.1 (C(3′) and C(5′)), 131.1 (C(1)), 134.7 (C(1′)), 142.1 (C(4)), 146.2 (CH=N$^+$),154.4 (C(3) and C(5)), 169.5 (CO). ESI/MS *m/z* (%): 415 (M$^+$+H, 100). ESI/HRMS calcd for $C_{23}H_{31}N_2O_5$ (M$^+$+H): 415.2227, found 415.2229.

α-5-(3,4,5-Trimethoxybenzamido)pentyl-*N*-cyclohexyl nitrone (40). η = 69%. ^{1}H NMR (CD_3OD): δ = 1.22–1.91 (16H, *m*, $N(CH_2)_2(\underline{C}H_2)_3$ and $N^+CH(\underline{C}H_2)_5$), 2.44–2.51 (2H, *m*, $NCH_2\underline{C}H_2$), 3.39 (2H, *t*, *J* = 7.0 Hz, NCH_2), 3.74–3.79 (1H, *m*, N^+CH), 3.80 (3H, *s*, OCH_3), 3.89 (6H, *s*, 2 × OCH_3), 7.17 (2H, *s*, H(2) and H(6)), 7.20 (1H, *t*, *J* = 5.9 Hz, CH=N$^+$). ^{13}C NMR (CD_3OD): δ = 25.9 ($N^+CHCH_2\underline{C}H_2CH_2\underline{C}H_2$), 26.1 ($N^+CH(CH_2)_2\underline{C}H_2$ and $N(CH_2)_2\underline{C}H_2$), 27.5 ($N(CH_2)_3\underline{C}H_2$), 27.8 ($NCH_2\underline{C}H_2$), 30.1 ($N(CH_2)_4\underline{C}H_2$), 31.9 ($N^+CH\underline{C}H_2(CH_2)_3\underline{C}H_2$), 40.8 ($NCH_2$), 56.7 (2 × OCH_3), 61.1 (OCH_3), 74.6 (N^+CH), 106.0 (C(2) and C(6)), 131.1 (C(1)), 142.1 (C(4)), 144.2 (CH=N$^+$), 154.5 (C(3) and C(5)), 169.5 (CO). ESI/MS *m/z* (%): 407 (M$^+$+H, 8), 195 (100). ESI/HRMS calcd for $C_{22}H_{35}N_2O_5$ (M$^+$+H): 407.2540, found 407.2534.

α-7-(3,4,5-Trimethoxybenzamido)heptyl-*N*-*tert*-butyl nitrone (41). η = 82%. ^{1}H NMR (CD_3OD): δ = 1.35–1.44 (6H, *m*, $N(CH_2)_2(\underline{C}H_2)_2CH_2\underline{C}H_2$), 1.47 (9H, *s*, $C(\underline{C}H_3)_3$), 1.53–1.66 (4H, *m*, $N(CH_2)_4\underline{C}H_2CH_2\underline{C}H_2$), 2.42–2.49 (2H, *m*, $NCH_2\underline{C}H_2$), 3.37 (2H, *t*, *J* = 7.3 Hz, NCH_2), 3.80 (3H, *s*, OCH_3), 3.89 (6H, *s*, 2 × OCH_3), 7.16 (1H, *s*, H(2) and H(6)), 7.24 (1H, *t*, *J* = 5.7 Hz, CH=N$^+$). ^{13}C NMR (CD_3OD): δ = 26.3 ($N(CH_2)_2\underline{C}H_2$), 27.9 ($N(CH_2)_5\underline{C}H_2$), 28.0 ($C(\underline{C}H_3)_3$), 28.3 ($N(CH_2)_3\underline{C}H_2$), 30.1 ($N(CH_2)_4\underline{C}H_2$), 30.5 ($NCH_2\underline{C}H_2$), 30.6 ($N(CH_2)_6\underline{C}H_2$), 41.1 ($NCH_2$), 56.7 (2 × OCH_3), 61.1 (OCH_3), 70.5 ($\underline{C}(CH_3)_3$), 105.9 (C(2) and C(6)), 131.2 (C(1)), 142.0 (C(4)), 142.3 (CH=N$^+$), 154.4 (C(3) and C(5)), 169.5 (CO). ESI/MS *m/z* (%): 431 (M$^+$+Na, 3), 400 (37), 195 (83), 154 (100). ESI/HRMS calcd for $C_{22}H_{36}N_2O_5Na$ (M$^+$+Na): 431.2516, found 431.2505.

α-9-(3,4,5-Trimethoxybenzamido)nonyl-*N*-*tert*-butyl nitrone (42). η = 69%. ^{1}H NMR (CD_3OD): δ = 1.31–1.43 (10H, *m*, $N(CH_2)_2(\underline{C}H_2)_4CH_2\underline{C}H_2$), 1.47 (9H, *s*, $C(\underline{C}H_3)_3$), 1.52–1.65 (4H, *m*, $N(CH_2)_6\underline{C}H_2CH_2\underline{C}H_2$), 2.41–2.48 (2H, *m*, $NCH_2\underline{C}H_2$), 3.36 (2H, *t*, *J* = 7.2 Hz, NCH_2), 3.80 (3H, *s*, OCH_3), 3.89 (6H, *s*, 2 × OCH_3), 7.16 (2H, *s*, H(2) and H(6)), 7.24 (1H, *t*, *J* = 5.7 Hz, CH=N$^+$). ^{13}C NMR (CD_3OD): δ = 26.4 ($N(CH_2)_2\underline{C}H_2$), 28.0 ($C(\underline{C}H_3)_3$), 28.1 ($N(CH_2)_7\underline{C}H_2$), 28.3 ($N(CH_2)_3\underline{C}H_2$), 30.3 ($N(CH_2)_6\underline{C}H_2$), 30.4 ($N(CH_2)_4\underline{C}H_2$), 30.5 ($NCH_2\underline{C}H_2(CH_2)_3\underline{C}H_2$), 30.6 ($N(CH_2)_8\underline{C}H_2$), 41.2 ($NCH_2$), 56.7 (2 × OCH_3), 61.1 (OCH_3), 70.5 ($\underline{C}(CH_3)_3$), 105.9 (C(2) and C(6)), 131.2 (C(1)), 142.0 (C(4)), 142.4 (CH=N$^+$), 154.4 (C(3) and C(5)), 169.4 (CO). ESI/MS *m/z* (%): 459 (M$^+$+Na, 3), 437 (M$^+$+H, 2), 428 (26), 195 (87), 154 (100). ESI/HRMS calcd for $C_{24}H_{41}N_2O_5$ (M$^+$+H): 437.3010, found 437.3004.

4.2. Pharmacology

4.2.1. Evaluation of acetyl and butyrylcholinesterase inhibitory activity

The inhibitory activity of compounds under study on AChE and BChE was evaluated following the Ellman's method [15] (see SI).

4.2.2. Evaluation of AChE kinetics and AChE-inhibitor kinetics

To determine the steady-state kinetic parameters (K_m, Michaelis constant and V_{max}, maximum rate) of AChE, their enzymatic activities were evaluated in the presence of different ATCI concentrations (see SI). To evaluate the mechanism of AChE inhibition of the most promising compounds (**33** and **38**) substrate-dependent kinetic experiments were also performed (see SI).

4.2.3. Evaluation of cytotoxicity/antioxidant outline in cell-based assays

4.2.3.1. Cell lines and culture conditions. SH-SY5Y cells (ATCC, Manassas, VA, USA), a human neuroblastoma cell line [41,42], and HepG2 (ECACC, UK), a human hepatocellular carcinoma cell line were used (see SI).

4.2.3.2. Cytotoxicity screening and cell viability assays. Differentiated SH-SY5Y and HepG2 cells were exposed to increased concentrations of the test compounds (1, 10 and 50 μM) in cell culture medium for 24 h or 48 h, respectively. The cytotoxic endpoints (MTT and reasazurin reduction assays) are described in literature [38,43] and in SI.

4.2.3.3. Cellular antioxidant screening. The nitrones' antioxidant differentiated efficiency in the presence of an oxidative stressor was evaluated using SH-SY5Y cells treated with nitrones **33** and **38** at different concentrations (10, 50 and 100 μM). Cellular oxidative damage was induced by the incubation of different OS-induced agents, namely hydrogen peroxide (H_2O_2 1 mM for 4 h), *tert*-butyl hydroperoxide (*t*-BHP 200 μM for 4 h); rotenone and antimycin A (ROT/AA 1 μM for 4 h); and doxorubicin (DOX 1 μM for 4 h). Two protocols have been used: a) the tested compounds were pre-incubated for 24 h and then pro-oxidant agents were added to the cell culture; and b) the pro-oxidant agents were first added to the cell culture and then the tested compounds were incubated for 24 h. After incubation time, cellular metabolic activity was determined using the resazurin reduction assay [43].

4.3. Data analysis

Data analysis for all the studies are specified in SI.

4.4. Molecular modelling studies

4.4.1. Ligands conformational analysis

Nitrone compounds **27**–**35**, **38**–**40**, and Donepezil enantiomers 3D structures were built and optimised using the Maestro GUI [44]. All molecules were submitted to 5000 steps of Monte Carlo conformational search as implemented in MacroModel [45]. Conformers were generated by randomly moving rotatable bonds and resulting geometries were optimised using 2500 iteration of the Polack Ribiere Conjugate Gradient algorithm and energy evaluated by means of the OPLS3 force field [46]. Water environment effects were mimicked according to GB/SA implicit solvation model. The global minimum of each molecule was submitted to docking simulations.

4.4.2. Docking simulation studies

Target models of AChE and BChE were designed starting from Protein Data Bank (PDB) [47] crystallographic structures 4EY7 [48] and 1P0I [49], respectively. The original PDB entries were selected taking into account the organism of provenience (*Homo sapiens*), the best available X-ray resolution and, in the case of 4EY7, the co-crystallised ligand (Donepezil). In order to add hydrogen atoms and missing residues, and to remove water molecules, before being used in docking simulation both target models were submitted to the Protein Preparation Wizard [50]. According to Glide docking software [51–54] the binding site was defined by means of a 27,000 $Å^3$ large regular box centred onto the catalytic Ser residue 203 and 198 for *h*AChE and *h*BChE models, respectively. Flexible ligand docking algorithm at extra precision level (XP) was adopted for exploring the recognition properties of compounds **27**–**35** and **38**–**40**. The binding free energy was estimated by the MM-GBSA method. Solvent effects were mimicked by the VSGB 2.0 continuum dielectric model [55], as implemented in Prime [56].

4.4.3. Pan Assay INterference compoundS (PAINS) evaluation

FAF4-Drug [57,58] and ZINC PAINS Pattern Identifier [59] web services were used to theoretically explore the PAINS properties of the chemical structures of the investigated compounds. Both methods did not highlight any issue related to the molecules under study.

Acknowledgements

This work was funded by FEDER funds through the Operational Programme Competitiveness Factors-COMPETE and national funds by FCT – Foundation for Science and Technology under research grants (QUI/UI0081/2013, NORTE-01-0145-FEDER-000028, POCI-01-0145-FEDER-016659, and PTDC/DTP-FTO/2433/2014). C. Oliveira (SFRH/BD/88773/2012, NORTE-01-0145-FEDER-000028), F. Cagide (SFRH/BPD/74491/2010, NORTE-01-0145-FEDER-000028), J. Teixeira (PTDC/DTP-FTO/2433/2014, NORTE-01-0145-FEDER-000028) grants are supported by FCT, POPH and QREN. This article is based upon work supported by the COST Action CA15135.

Appendix A. Supplementary data

Supplementary data to this article can be found online at https://doi.org/10.1016/j.ejmech.2019.04.026.

References

[1] R. Fang, S. Ye, J. Huangfu, D.P. Calimag, Music therapy is a potential intervention for cognition of Alzheimer's disease: A mini-review, Transl. Neurodegener. 6 (2017) 2. https://doi.org/10.1186/s40035-017-0073-9.
[2] S. Arun, L. Liu, G. Donmez, Mitochondrial biology and neurological diseases, Curr. Neuropharmacol. 14 (2016) 143–154. https://doi.org/10.2174/1570159X13666150703154541.
[3] M.S. Cazarim, J.C. Moriguti, A.T. Ogunjimi, L.R. Pereira, Perspectives for treating Alzheimer's disease: A review on promising pharmacological substances, Sao Paulo Med. J. 134 (2016) 342–354. https://doi.org/10.1590/1516-3180.2015.01980112.
[4] C. Guo, L. Sun, X. Chen, D. Zhang, Oxidative stress, mitochondrial damage and neurodegenerative diseases, Neural. Regen. Res. 8 (2013) 2003–2014. https://doi.org/10.3969/j.issn.1673-5374.2013.21.009.
[5] H. Zheng, M. Fridkin, M. Youdim, From single target to multitarget/network therapeutics in Alzheimer's therapy, Pharmaceuticals 7 (2014) 113–135. https://doi.org/10.3390/ph7020113.
[6] A. Talevi, Multi-target pharmacology: Possibilities and limitations of the "skeleton key approach" from a medicinal chemist perspective, Front. Pharmacol. 6 (2015) 205. https://doi.org/10.3389/fphar.2015.00205.
[7] K. Nikolic, L. Mavridis, T. Djikic, J. Vucicevic, D. Agbaba, K. Yelekci, J.B.O. Mitchell, Drug design for CNS diseases: Polypharmacological profiling of compounds using cheminformatic, 3D-QSAR and virtual screening methodologies, Front. Neurosci. 10 (2016) 265. https://doi.org/10.3389/fnins.2016.00265.
[8] A. Kumar, A. Singh, Ekavali, A review on Alzheimer's disease pathophysiology and its management: An update, Pharmacol. Rep. 67 (2015) 195–203. https://doi.org/10.1016/j.pharep.2014.09.004.
[9] A.A. Shah, T.A. Dar, P.A. Dar, S.A. Ganie, M.A. Kamal, A current perspective on the inhibition of cholinesterase by natural and synthetic inhibitors, Curr. Drug Metabol. 18 (2017) 96–111. https://doi.org/10.2174/1389200218666161123122734.
[10] M.B. Čolović, D.Z. Krstić, T.D. Lazarević-Pašti, A.M. Bondžić, V.M. Vasić, Acetylcholinesterase inhibitors: Pharmacology and toxicology, Curr. Neuropharmacol. 11 (2013) 315–335. https://doi.org/10.2174/1570159X11311030006.
[11] P. Anand, B. Singh, A review on cholinesterase inhibitors for Alzheimer's disease, Arch Pharm. Res. (Seoul) 36 (2013) 375–399. https://doi.org/10.1007/s12272-013-0036-3.
[12] Q. Li, H. Yang, Y. Chien, H. Sun, Recent progress in the identification of selective butyrylcholinesterase inhibitors for Alzheimer's disease, Eur. J. Med. Chem. 132 (2017) 294–309. https://doi.org/10.1016/j.ejmech.2017.03.062.
[13] D.G. Wilkinson, P.T. Francis, E. Schwam, J. Payne-Parrish, Cholinesterase inhibitors used in the treatment of Alzheimer's disease: The relationship between pharmacological effects and clinical efficacy, Drugs Aging 21 (2004) 453–478. https://doi.org/10.2165/00002512-200421070-00004.
[14] Z.Y. Wang, J.G. Liu, H. Li, H.M. Yang, Pharmacological effects of active components of Chinese herbal medicine in the treatment of Alzheimer's disease: A review, Am. J. Chin. Med. 44 (2016) 1525–1541. https://doi.org/10.1142/S0192415X16500853.
[15] C. Oliveira, F. Cagide, J. Teixeira, R. Amorim, L. Sequeira, F. Mesiti, T. Silva, J. Garrido, F. Remião, S. Vilar, E. Uriarte, P.J. Oliveira, F. Borges, Hydroxybenzoic acid derivatives as dual-target ligands: Mitochondriotropic antioxidants and cholinesterase inhibitors, Front. Chem. 6 (2018) 126. https://doi.org/10.3389/fchem.2018.00126.
[16] A.R. Green, T. Ashwood, T. Odergren, D.M. Jackson, Nitrones as neuroprotective agents in cerebral ischemia, with particular reference to NXY-059, Pharmacol. Ther. 100 (2003) 195–214. https://doi.org/10.1016/j.pharmthera.2003.07.003.
[17] M.C. Krishna, W. Degraff, O.H. Hankovsky, C.P. Sár, T. Kálai, J. Jekő, A. Russo, J.B. Mitchell, K. Hideg, Studies of structure–activity relationship of nitroxide free radicals and their precursors as modifiers against oxidative damage, J. Med. Chem. 41 (1998) 3477–3492. https://doi.org/10.1021/jm9802160.
[18] C. Oliveira, S. Benfeito, C. Fernandes, F. Cagide, T. Silva, F. Borges, NO- and HNO-donors, nitrones, and nitroxides: Past, present and future, Med. Res. Rev. 38 (2017) 1159–1187. https://doi.org/10.1002/med.21461.
[19] J.S. Modica-Napolitano, K. Singh, Mitochondria as targets for detection and treatment of cancer, Expert Rev. Mol. Med. 4 (2002) 1–19. https://doi.org/10.1017/S1462399402004453.
[20] G.L. Ellman, K.D. Courtney, V. Andres, R.M. Featherstone, A new and rapid colorimetric determination of acetylcholinesterase activity, Biochem. Pharmacol. 7 (1961) 88–95. https://doi.org/10.1016/0006-2952(61)90145-9.
[21] S. Di Giovanni, A. Borloz, A. Urbain, A. Marston, K. Hostettmann, P.-A. Carrupt, M. Reist, In vitro screening assays to identify natural or synthetic acetylcholinesterase inhibitors: Thin layer chromatography versus microplate methods, Eur. J. Pharm. Sci. 33 (2008) 109–119. https://doi.org/10.1016/j.ejps.2007.10.004.
[22] C.A. Lipinski, F. Lombardo, B.W. Dominy, P.J. Feeney, Experimental and computational approaches to estimate solubility and permeability in drug discovery and development settings, Adv. Drug Deliv. Rev. 46 (2001) 3–26. https://doi.org/10.1016/S0169-409X(00)00129-0.
[23] P.D. Leeson, B. Springthorpe, The influence of drug-like concepts on decision-making in medicinal chemistry, Nat. Rev. Drug Discov. 6 (2007) 881–890.

https://doi.org/10.1038/nrd2445.
[24] D.E. Clark, Rapid calculation of polar molecular surface area and its application to the prediction of transport phenomena. 2. Prediction of blood-brain barrier penetration, J. Pharm. Sci. 88 (1999) 815–821. https://doi.org/10.1021/js980402t.
[25] H. Pajouhesh, G.R. Lenz, Medicinal chemical properties of successful central nervous system drugs, NeuroRx 2 (2005) 541–553. https://doi.org/10.1602/neurorx.2.4.541.
[26] S.A. Hitchcock, L.D. Pennington, Structure–brain exposure relationships, J. Med. Chem. 49 (2006) 7559–7583. https://doi.org/10.1021/jm060642i.
[27] C.W. Fong, Permeability of the blood-brain barrier: Molecular mechanism of transport of drugs and physiologically important compounds, J. Membr. Biol. 248 (2015) 651–669. https://doi.org/10.1007/s00232-015-9778-9.
[28] Z. Rankovic, CNS drug design: Balancing physicochemical properties for optimal brain exposure, J. Med. Chem. 58 (2015) 2584–2608. https://doi.org/10.1021/jm501535r.
[29] S. Genheden, U. Ryde, The MM/PBSA and MM/GBSA methods to estimate ligand-binding affinities, Expert Opin. Drug Discov. 10 (2015) 449–461. https://doi.org/10.1517/17460441.2015.1032936.
[30] T.L. Rosenberry, X. Brazzolotto, I.R. Macdonald, M. Wandhammer, M. Trovaslet-Leroy, S. Darvesh, F. Nachon, Comparison of the binding of reversible inhibitors of human butyrylcholinesterase and acetylcholinesterase: A crystallographic, kinetic and calorimetric study, Molecules 22 (2017) 1–21. https://doi.org/10.3390/molecules22122098.
[31] D.C. Vellom, A. Radić, Y. Li, N.A. Pickering, S. Camp, P. Taylor, Amino acids residues controlling acetylcholinesterase and butyrylcholinesterase specificity, Biochemistry 32 (1993) 12–17. https://doi.org/10.1021/bi00052a003.
[32] G. Johnson, S.W. Moore, The peripheral anionic site of acetylcholinesterase: Structure, functions and potential role in rational drug design, Curr. Pharmaceut. Des. 12 (2006) 217–225. https://doi.org/10.2174/138161206775193127.
[33] H. Dvir, I. Silman, M. Harel, T.L. Rosenberry, J.L. Sussman, Acetylcholinesterase: From 3D structure to function, Chem. Biol. Interact. 197 (2010) 10–22. https://doi.org/10.1016/j.cbi.2010.01.042.
[34] H. Sugimoto, H. Ogura, Y. Arai, Y. Limura, Y. Yamanishi, Research and development of donepezil hydrochloride, a new type of acetylcholinesterase inhibitor, Jpn. J. Pharmacol. 89 (2002) 7–20. https://doi.org/10.1254/jjp.89.7.
[35] M. Pohanka, Inhibitors of acetylcholinesterase and butyrylcholinesterase meet immunity, Int. J. Mol. Sci. 15 (2014) 9809–9825. https://doi.org/10.3390/ijms15069809.
[36] J.M. Berg, J.L. Tymoczko, S. Lubert, Biochemistry, W H Freeman, New York, 2002.
[37] Z. Lin, Y. Will, Evaluation of drugs with specific organ toxicities in organ-specific cell lines, Toxicol. Sci. 126 (2012) 114–127. https://doi.org/10.1093/toxsci/kfr339.
[38] D. Lobner, Comparison of the LDH and MTT assays for quantifying cell death: validity for neuronal apoptosis? J. Neurosci. Methods 96 (2000) 147–152. https://doi.org/10.1016/S0165-0270(99)00193-4.
[39] J. Teixeira, C. Oliveira, R. Amorim, F. Cagide, J. Garrido, J.A. Ribeiro, C.M. Pereira, A.F. Silva, P.B. Andrade, P.J. Oliveira, F. Borges, Development of hydroxybenzoic-based platforms as a solution to deliver dietary antioxidants to mitochondria, Sci. Rep., Nature 7 (2017) 6842. https://doi.org/10.1038/s41598-017-07272-y.
[40] G. Glaros, Oxidation of primary alcohols to aldehydes with pyridinium chlorochromate. An organic chemistry experiment, J. Chem. Educ. 55 (1978) 410. https://doi.org/10.1021/ed055p410.
[41] C. Fernandes, M. Pinto, C. Martins, M.J. Gomes, B. Sarmento, P.J. Oliveira, F. Remiao, F. Borges, Development of a PEGylated-based platform for efficient delivery of dietary antioxidants across the blood–brain barrier, Bioconjug. Chem. 29 (2018) 1677–1689. https://doi.org/10.1021/acs.bioconjchem.8b00151.
[42] D.J. Barbosa, J.P. Capela, R. Silva, V. Vilas-Boas, L.M. Ferreira, P.S. Branco, E. Fernandes, M.d.L. Bastos, F. Carvalho, The mixture of “ecstasy” and its metabolites is toxic to human SH-SY5Y differentiated cells at in vivo relevant concentrations, Arch. Toxicol. 88 (2014) 455–473. https://doi.org/10.1007/s00204-013-1120-7.
[43] F.S. Silva, I.G. Starostina, V.V. Ivanova, A.A. Rizvanov, P.J. Oliveira, S.P. Pereira, Determination of metabolic viability and cell mass using a Tandem Resazurin/Sulforhodamine B assay, Curr. Protoc. Toxicol. 68 (2016) 2.24.1–2.24.15. https://doi.org/10.1002/cptx.1.
[44] Maestro Version 10.7, Schrödinger LLC, New York (USA), 2016.
[45] MacroModel Version 11.3, Schrödinger LLC, New York (USA), 2016.
[46] E. Harder, W. Damm, J. Maple, C. Wu, M. Reboul, J.Y. Xiang, L. Wang, D. Lupyan, M.K. Dahlgren, J.L. Knight, J.W. Kaus, D.S. Cerutti, G. Krilov, W.L. Jorgensen, R. Abel, R.A. Freisner, OPLS3: a force field providing broad coverage of drug-like small molecules and proteins, J. Chem. Theory Comput. 12 (2016) 281–296. https://doi.org/10.1021/acs.jctc.5b00864.
[47] H.M. Berman, J. Westbrook, Z. Feng, G. Gilliland, T.N. Bhat, H. Weissig, I.N. Shindyalov, P.E. Bourne, The protein data bank, Nucleic Acids Res. 28 (2000) 235–242. https://doi.org/10.1093/nar/28.1.235.
[48] J. Cheung, M.J. Rudolph, F. Burshteyn, M.S. Cassidy, E.N. Gary, J. Love, M.C. Franklin, J.J. Height, Structures of human acetylcholinesterase in complex with pharmacologically important ligands, J. Med. Chem. 55 (2012) 10282–10286. https://doi.org/10.1021/jm300871x.
[49] Y. Nicolet, O. Lockridge, P. Masson, J.C. Fontecilla-Camps, F. Nachon, Crystal structure of human butyrylcholinesterase and of its complexes with substrate and products, J. Biol. Chem. 278 (2003) 41141–41147. https://doi.org/10.1074/jbc.M210241200.
[50] G.M. Sastry, M. Adzhigirey, T. Day, R. Annabhimoju, W. Sherman, Protein and ligand preparation: Parameters, protocols, and influence on virtual screening enrichments, J. Comput. Aided Mol. Des. 27 (2013) 221–234. https://doi.org/10.1007/s10822-013-9644-8.
[51] Schrödinger Glide, LLC, New York, USA, 2018.
[52] R.A. Friesner, R.B. Murphy, M.P. Repasky, L.L. Frye, J.R. Greenwood, T.A. Halgren, P.C. Sanschagrin, D.T. Mainz, Extra precision glide: Docking and scoring incorporating a model of hydrophobic enclosure for protein-ligand complexes, J. Med. Chem. 49 (2006) 6177–6196. https://doi.org/10.1021/jm051256o.
[53] T.A. Halgren, R.B. Murphy, R.A. Friesner, H.S. Beard, L.L. Frye, W.T. Pollard, J.L. Banks, Glide: A new approach for rapid, accurate docking and scoring. 2. Enrichment factors in database screening, J. Med. Chem. 47 (2004) 1750–1759. https://doi.org/10.1021/jm030644s.
[54] R.A. Friesner, J.L. Banks, R.B. Murphy, T.A. Halgren, J.J. Klicic, D.T. Mainz, M.P. Repasky, E.H. Knoll, M. Shelley, J.K. Perry, D.E. Shaw, P. Francis, P.S. Shenkin, Glide: A new approach for rapid, accurate docking and scoring. 1. Method and assessment of docking accuracy, J. Med. Chem. 47 (2004) 1739–1749. https://doi.org/10.1021/jm0306430.
[55] J. Li, R. Abel, K. Zhu, Y. Cao, S. Zhao, R.A. Friesner, The VSGB 2.0 model: A next generation energy model for high resolution protein structure modelling, Proteins 79 (2011) 2794–2812. https://doi.org/10.1002/prot.23106.
[56] Schrödinger Prime, LLC, New York, USA, 2018.
[57] D. Lagorce, O. Sperandio, H. Galons, M.A. Miteva, B.O. Villoutreix, FAF-Drugs2: Free ADME/tox filtering tool to assist drug discovery and chemical biology projects, BMC Bioinf. 9 (2008) 396. https://doi.org/10.1186/1471-2105-9-396.
[58] http://fafdrugs3.mti.univ-paris-diderot.fr.
[59] http://zinc15.docking.org/patterns/home.